warrants future genetic analysis in schizophrenia based in its complimentary pattern of expression with netrin G1.[17]

In conclusion, our data suggest the possible involvement of human netrin G1 or a nearby gene in the vulnerability to schizophrenia.

Acknowledgements

We are grateful to all participants in this study.

References

1. Gottesman II. Schizophrenia Genesis. New York: W.H. Freeman & Company, 1991
2. Murray RM and Lewis SW. Is schizophrenia a neurodevelopmental disorder? British Medical Journal Clinical Research Ed. 1987;295:681-2.
3. Tessier-Lavigne M, Goodman CS. The molecular biology of axon guidance. Science 1966;274:1123-1133.
4. Ishii N, Wadsworth WG, Stern BD, et al. UNC-6, a laminin-related protein, guides cell and pioneer axon migrations in *C. elegans*. Neuron 1992;9:873-881.
5. Serafini T, Kennedy TE, Galko MJ, et al. The netrins define a family of axon outgrowth-promoting proteins homologous to *C. elegans UNC-6*. Cell 1994;78:409-424.
6. Hutter H, Vogel BE, Plenefisch JD, et al. Conservation and novelty in the evolution of cell adhesion and extracellular matrix genes. Science 2000;287:989-994.
7. Nakashiba T, Ikeda T, Nishimura S, et al. Netrin-G1 a novel glycosyl phosphatidylinositol-linked mammalian netrin that is functionally divergent from classical netrins. J Neurosci 2000;20:6540-6550.
8. Yu TW, Bargmann CI. Dynamic regulation of axon guidance. Nat Neurosci 2001;Suppl 4:1169-1176.
9. Ranade K, Chang MS, Ting CT, et al. High-throughput genotyping with single nucleotide polymorphisms. Genome Res 2001;11:1262-1268.
10. Dudbridge F, Koeleman BP, Todd JA, et al. Unbiased application of the transmission/disequilibrium test to multilocus haplotypes. Am J Hum Genet 2000;66:2009-2012.
11. Abecasis GR, Cookson WO. GOLD-graphical overview of linkage disequilibrium. Bioinformatics 2000;16:182-183.
12. Darian-Smith I, Galea MP, Darian-Smith C, et al. The anatomy of manual dexterity: the new connectivity of the primate sensorimotor thalamus and cerebral cortex. Adv Anat Cell Biol 1996;133:1-142.
13. Braff DL, Geyer MA, Swerdlow NR. Human studies of prepulse inhibition of startle: normal subjects, patient groups, and pharmacological studies. Psychopharmacology 2001;156: 234-258.
14. Geyer MA, Krebs-Thomson K, Braff DL, et al. Pharmacological studies of prepulse inhibition models of sensorimotor gating deficits in schizophrenia: a decade in review. Psychopharmacology 2001;156:117-154.
15. Abecasis GR, Noguchi E, Heinzmann A, et al. Extent and distribution of linkage disequilibrium in three genomic regions. Am J Hum Genet 2001;68:191-197.
16. Nakajima T, Jorde LB, Ishigami T, et al. Nucleotide diversity and haplotype structure of the human angiotensin gene in two populations. Am J Hum Genet 2002;70:108-123.
17. Nakashiba T, Nishimura S, Ikeda T, et al. Complementary expression and neurite outgrowth activity of netrin-G subfamily members. Mech Dev 2002;111:47-60.

THE JOURNAL OF BIOLOGICAL CHEMISTRY
Vol. 279, No. 44, Issue of October 29, pp. 45773–45781, 2004
Printed in U.S.A.

Neuronal Functions of the Novel Serine/Threonine Kinase Ndr2*

Received for publication, March 31, 2004, and in revised form, July 6, 2004
Published, JBC Papers in Press, August 12, 2004, DOI 10.1074/jbc.M403552200

Oliver Stork‡§, Alexander Zhdanov‡, Alexei Kudersky‡, Takeo Yoshikawa¶, Kunihiko Obata‖, and Hans-Christian Pape‡**

From the ‡Institute of Physiology, Otto-von-Guericke University Magdeburg, D-39120 Magdeburg, Germany, the ¶Laboratory of Molecular Psychiatry, Brain Science Institute of RIKEN, 2-1 Hirosawa, Wako 351-0198, Japan, and the ‖Laboratory of Neurochemistry, National Institute for Physiological Sciences, Okazaki 444-8585, Japan

We have identified a novel member of the Ndr subfamily of serine/threonine protein kinases, Ndr2, as a gene product that is induced in the mouse amygdala during fear memory consolidation and examined a possible function of this kinase in neural differentiation. Expression of *Ndr2* mRNA was detected in various cortical and subcortical brain regions, as well as non-neuronal tissues. Its expression in the amygdala was increased 6 h after Pavlovian fear conditioning training and returned to control levels within 24 h. To study intracellular localization and functions of Ndr2, EGFP::Ndr2 fusion proteins were expressed in rat pheochromocytoma (PC12) cells and acutely isolated cortical neurons, thereby revealing an association of Ndr2 with the actin cytoskeleton in somata, neurites and filopodia, in spines and at sites of cell contact. Co-precipitation and pull-down experiments support this finding. Evidence for an involvement of Ndr2 in actin-mediated cellular functions further comes from the observation of decreased cell spreading and changes in neurite outgrowth that were associated with protein serine phosphorylation in transfected PC12 cells. Together, our data suggest that Ndr2 is an interesting candidate gene for the regulation of structural processes in differentiating and mature neuronal cells.

Stimulus-dependent modifications of cell structure and connectivity in the central nervous system are basic elements of long term memory formation. Protein kinases and protein phosphatases are key regulators of these processes, which they control and co-ordinate through the phosphorylation and/or dephosphorylation of neurotransmitter receptors and ion channels, cytoskeleton elements, cell surface molecules, and transcription factors (1).

We have employed a classic fear conditioning paradigm to isolate candidate genes involved in memory-related functions in the brain (2). Fear conditioning is highly amenable to cellular and molecular approaches to learning and memory, because conditioned subjects (*a*) very quickly learn to associate a previously neutral sensory stimulus (conditional stimulus) and an aversive, unconditional stimulus during fear conditioning training and (*b*) develop a robust and easily measurable long term memory after a single training session. Moreover, the neuronal circuits and cellular mechanisms that underlie classic fear conditioning have been investigated in detail (reviewed in Ref. 3). These conceptual and technical advantages have allowed researchers to show that, among other factors, protein kinase A, mitogen-activated protein kinase and calcium/calmodulin-dependent kinases are critical for fear conditioning (summarized in Ref. 4). Some of these protein kinase activities could even be tracked down to the amygdala (5–7). Recent evidence further suggests an involvement of Rho-mediated signaling pathways and the Rho-associated kinase ($p160^{ROCK}$) in amygdala plasticity after fear conditioning (8). This pathway may be of particular importance, because it controls actin-mediated changes in dendrite and spine morphology, which are key elements of structural plasticity and memory consolidation (9, 10).

Screening of a subtracted library from the amygdala of fear-conditioned animals has now led us to the identification of a novel serine/threonine kinase, Ndr2 (also known as serine/threonine kinase 38-like protein, STK38l). The novel kinase belongs to the nuclear Dbf2-related (Ndr)[1] subfamily of serine/threonine kinases that control cell division and morphogenesis in various cell types, including neurons, and is distantly related to $p160^{ROCK}$. Ndr2 has in parallel been identified through homology cloning (11), and activation through S100B and Mob (Mps one binder) proteins with subsequent autophosphorylation has been described in two recent reports (12, 13). In the current study we have begun to investigate possible neuronal functions of this kinase. To this end, we studied the expression of Ndr2 in the brain and its induction in various brain areas during consolidation of Pavlovian fear memory. We furthermore provide evidence for interaction of Ndr2 with the actin cytoskeleton and its involvement in neuronal growth and differentiation in cultured PC12 cells.

EXPERIMENTAL PROCEDURES

A fragment of the 3′-untranslated region of the Ndr2 mRNA (clone #VIIE6) was identified through suppression subtractive hybridization of cDNA from the amygdala of fear-conditioned and control mice (Fig. 1*A*) und subsequent screening with cDNA blots (Fig. 1*B*). Experiments employed for the identification and expression analysis of clone #VIIE6 have been described previously (2). All animal experiments were performed in accordance with regulations through Japanese and German

* This work was supported by grants from the Deutsche Forschungsgemeinschaft (Leibniz-Program to H.-C. P.) and the Kultusministerium des Landes Sachsen Anhalt (to H.-C. P.), the Ministry of Education, Science, Sport and Culture (to K. O.), and an S&T fellowship from the European Union (to O. S.). The costs of publication of this article were defrayed in part by the payment of page charges. This article must therefore be hereby marked "*advertisement*" in accordance with 18 U.S.C. Section 1734 solely to indicate this fact.

The nucleotide sequence(s) reported in this paper has been submitted to the GenBank™/EBI Data Bank with accession number(s) AY223819.

** Present address: Neural Circuit Mechanisms Group, Brain Science Institute of RIKEN, 2-1 Hirosawa, Wako 351-0198, Japan.

§ To whom correspondence should be addressed. Tel.: 49-391-611-7130; Fax: 49-391-671-5819; E-mail: oliver.stork@medizin.uni-magdeburg.de.

[1] The abbreviations used are: Ndr, nuclear Dbf2-related subfamily; RACE, rapid amplification of cDNA ends; MOPS, 3-(*N*-morpholino)propanesulfonic acid; PBS, phosphate-buffered saline; MBP, myelin basic protein; Ab, antibody; GFP, green fluorescent protein; EGFP, enhanced GFP; NGF, nerve growth factor; CRE, cyclic AMP-responsive element.

law and were approved by the Committee for Animal Research, Okazaki National Institutes (permission NRS A11-82-3 and A11-82-65) and the Regierungspräsidium Dessau (2-375 UNI MD).

Cloning and Sequencing of Full-length Ndr2—Clone #VIIE6 was sequenced using the Thermo Sequenase cycle sequencing system (Amersham Biosciences) according to the manufacturer's protocols. In brief, 1 μg of cDNA was amplified in the presence of fluorescence-labeled M13 forward or reverse primer oligonucleotide (Stratagene) and ddG, ddA, ddT, or ddC to terminate polymerization. Thirty cycles of 95 °C for 30 s, 50 °C for 30 s, and 70 °C for 60 s were applied. Products were loaded onto a polyacrylamide gel containing 7 M urea, separated at 2000 V, and detected in a DNA sequencer (Model 4000L, LI-COR Inc., Lincoln, NE). Based on the sequence information from clone #VIIE6, rapid amplification of cDNA ends (RACE) was done using the SMART RACE system (BD Bioscience). To this end, total RNA was isolated from mouse brain using RNeasy spin columns (Qiagen) and reverse-transcribed with Superscript II (Promega) in the presence of a modified oligo(dT) cDNA synthesis primer (for 3′-RACE) or oligo(dT) primer and SMART II oligonucleotide (for 5′-RACE). The 3′-end was amplified with a gene-specific primer oligonucleotide (5′-TCTGGAGATGTATGAAACCTGGGCTGTC-3′) and a universal primer mix (SMART RACE) in a touch down amplification procedure with 5 cycles of annealing for 10 s at 72 °C, 5 cycles at 70 °C, and 25 cycles of annealing at 68 °C, each preceded by denaturation for 5 s at 94 °C and followed by DNA polymerization for 3 min at 72 °C. For 5′-RACE, a gene-specific primer (5′-ATTCAAAGAGAGGATGTGCCAGGA-3′) was first used together with the universal primer mix for touch down amplification with 40 cycles in the final step. The product was diluted 1:50 and re-amplified with a nested gene-specific primer (5′-GGACAGCCCAGGTATCATACATCT-3′) and the nested universal primer (SMART RACE), using 29 cycles of 5 s at 94 °C, 10 s at 68 °C, and 3 min at 72 °C. RACE fragments were cloned into pGEM-Teasy and sequenced as described above. Sequences of three independent clones for each 3′-RACE and 5′-RACE were analyzed using Lasergene99 software (DNASTAR, Madison, WI) and NCBI and PROSITE databanks.

Chromosomal Localization—Two primers were derived from the 3′-untranslated region (5′-CACAGCTAAGTCTGGAGATGTA-3′, representing bp 3781–3802, and 5′-ATGATCATAGCAAAACAGTTGC-3′, representing bp 4193–4172) and used for radiation hybrid mapping with a mouse/hamster radiation hybrid panel (Invitrogen). Thirty cycles of denaturation (15 s at 94 °C), primer annealing (30 s at 60 °C), and synthesis (30 s at 72 °C) were applied, as described previously (14).

Northern Analysis—5 μg of total RNA was separated according to size with denaturing gel electrophoresis (in 20 mM MOPS, 5 mM sodium acetate, 1 mM EDTA, pH 7.0, containing 0.5 M formaldehyde), transferred to nylon membranes (Hybond-N, Amersham Biosciences), and fixed under UV light. *Ndr2* mRNA was visualized with Digoxigenin-labeled cRNA probes, generated through *in vitro* transcription from a vector containing either clone #VIIE6, the entire 5′-RACE product, or the coding region of the *Ndr2* cDNA (Fig. 1*A*), all of which produced consistent results, and subsequent chemiluminescence detection as described above.

Real-time PCR—Five 10-week-old male C57B/6J mice (M&B Taconic, Berlin, Germany) after extensive adaptation to the training apparatus (TSE Bad Homburg, Germany) were fear-conditioned with three conditional stimuli (10-kHz tone, 85 db for 10 s) that each co-terminated with an unconditional stimulus (0.6-mA foot shock, 1 s). Five pseudo-conditioned mice in parallel received explicitly unpaired presentation of these stimuli, and five controls each received three conditional stimuli, but no unconditional stimulus during training. Animals were returned to their home cages, and sacrificed 6 h later. Tissue samples from the basolateral complex of the amygdala, hippocampus, pre- and infralimbic ("prefrontal") cortex, and the cerebellar cortex were punched from 100-μm-thick coronal sections of freshly frozen brains. Total RNA was isolated, and first strand synthesis was done with Moloney murine leukemia virus reverse transcriptase in the presence of random decamer oligonucleotides (Ambion, Austin, TX). Samples were analyzed with TaqMan real-time PCR in an AbiPrism 7000. Ndr2 assays designed to analyze the exon borders at mRNA position 1219 and 1328 were used in triplicate experiments and controlled with assays for phosphoglycerate kinase and 18 S rRNA (assay-on-demand, Applied Biosystems).

In Situ Hybridization—Coronal and sagittal sections of 14-μm thickness were cut in a freezing microtome and thaw-mounted onto silane-coated slide glasses. Digoxigenin-labeled sense and antisense cRNA were generated from a clone containing the entire open reading frame of Ndr2 (Fig. 1*A*). *In situ* hybridization was performed with these probes as described previously (10). Briefly, after fixation in 4% *para*-formaldehyde in phosphate-buffered saline (PBS), sections were acetylated, dehydrated, and pre-hybridized for 2 h at room temperature. After hybridization over night and washing at 55 °C with 0.2× standard sodium citrate buffer containing 50% formamide, labeled cells were detected with alkaline phosphatase-coupled anti-digoxigenin antibody and subsequently stained using 4-nitro blue tetrazolium and 5-bromo-4-chloro-3-indolyl phosphate as substrate (all reagents from Roche Applied Science).

Purification of Ndr2 Protein—Fusion proteins of Ndr2 and the maltose binding protein (MBP::Ndr2) were generated using the pMAL vector system (New England Biolabs, Beverly, MA) according to the manufacturer's instructions. The coding region of *Ndr2* was amplified using primers 5′-ATGGCAATGACGGCAGGG-3′ and 5′-AGCACCCACTTCCTGTATTTC-3′ and cloned into vector pMAL-c2x. MBP::Ndr2 fusion proteins were expressed in *Escherichia coli* strain ER2508, sonified in 20 mM Tris, pH 7.4, containing 0.2 M NaCl, 1 mM EDTA, 0.02% NaN_3, and 0.5 mM phenylmethylsulfonyl fluoride, and pre-purified through chromatography on amylose columns (New England Biolabs). Ndr2 protein was then purified with affinity immuno-chromatography on Sepharose-coupled $Ab^{420-430}$ (see below). Samples were loaded in sodium phosphate buffer, pH 7.4, and eluted in 0.2 M glycine buffer, pH 2.8. The eluate was finally dialyzed against 20 mM sodium phosphate buffer, pH 7.4. For isolation of native Ndr2, brain samples were homogenized on ice with a 10-fold excess of 50 mM sodium phosphate buffer, pH 7.4, containing 0.15 M NaCl, 0.02% Triton X-100, 2 mM EDTA, and 0.02% NaN_3. After centrifugation at 300 × *g* to remove cell debris, the homogenate was applied to affinity chromatography with Sepharose-coupled $Ab^{420-430}$, eluted, and dialyzed as describe above.

Immunoblot Analysis—Polyclonal antibody $Ab^{420-430}$ was generated against peptide LQPVPNTTEPD coupled to keyhole limpet hemocyanin (Pineda Antibody Service, Berlin, Germany). Serum from an animal that detected both bacterially expressed and brain Ndr2 was selected and affinity-purified using the immunization peptide. Purified $Ab^{420-430}$ was used at a dilution of 1:500–1:1000 in immunoblot analysis. Antibodies to β-actin, β-tubulin, α-actinin (Sigma), synapsin I (Molecular Probes, Eugene, OR), phospho-serine (Qiagen), and neurofilament proteins (Biotrend Chemikalien, Köln, Germany) were used according to the manufacturer's recommendations. For immunoblot analysis, brain samples and cultured cells were homogenized in 1% SDS, 10 mM Tris-hydrochloride, pH 7.5, separated with electrophoresis on 8–10% polyacrylamide gels containing SDS, and transferred to nitrocellulose filters. After blocking of unspecific binding, blots were incubated with primary and horseradish peroxidase-coupled secondary antibodies (DAKO, Copenhagen Denmark) before visualization with "ECL-plus" substrate (Amersham Biosciences). $Ab^{420-430}$ detected native Ndr2 protein from the brain and MBP::Ndr2 fusion protein from bacteria at the predicted molecular masses of 54 and 96 kDa, respectively (Fig. 4*A*). The specificity of signals for Ndr2 and phospho-serine was confirmed through preincubation of primary antibodies with excess peptide LQPVPNTTEPD or MBP::Ndr2 fusion protein, or with *o*-phospho-L-serine, respectively.

Co-precipitation and Pull-down Assays—Protein samples for precipitation experiments were obtained from total brains, homogenized in 10-fold excess of 20 mM phosphate buffer, pH 7.4, containing 137 mM NaCl, 2.8 mM KCl, 0.5% Triton X-100, 0.02% NaN_3, 1 mM EDTA, 0.2 mM phenylmethylsulfonyl fluoride, and 1× Proteinase inhibitor mixture (Roche Molecular Biochemicals), or PC12 cells, homogenized in radioimmune precipitation assay buffer containing 50 mM Tris-HCl, pH 8.0, 150 mM NaCl, 10% glycerol, 1% IGEPAL CA-630, 0.5% sodium deoxycholate, 0.1% SDS, 1 mM phenylmethylsulfonyl fluoride, and Protease inhibitor mixture. For MBP::Ndr2 pull-down assays, 100 μg of the soluble protein fraction after centrifugation at 15,000 × *g* and clearing with amylose resin (New England Biolabs) were incubated with 2 μg of MBP::Ndr2 or 2 μg of MBP2 (New England Biolabs) for 1 h at 4 °C. After incubation for 90 min with amylose resin, MBP-amylose complexes were precipitated by centrifugation at 10,000 × *g*. For co-precipitation, protein samples were cleared with Sepharose-protein A/G (Amersham Pharmacia Biotech), and incubated with 5 μg of antibodies against actin or Ndr2 for 1 h at 4 °C. Complexes were precipitated with Sepharose-protein A/G at 4 °C for 1 h, centrifuged at 12,000 × *g*, then finally washed with radioimmune precipitation assay buffer and subsequently with 50 mM Tris-HCl, pH 8.0. Proteins precipitated in these ways were examined with SDS-PAGE and immunoblot analysis.

Immunohistochemistry—For immunohistochemical detection of Ndr2, freshly frozen coronal and sagittal sections of 14-μm thickness were used. Sections were fixed in 4% *para*-formaldehyde in PBS and washed in PBS, before unspecific binding was blocked with 3% bovine serum albumin, 10% rabbit normal serum, and 0.3% Triton X-100 in

PBS for 2 h. Ndr2 was detected with affinity-purified $Ab^{420-430}$ at a dilution of 1:300 to 1:500 in 3% bovine serum albumin, 2% rabbit normal serum, and PBS overnight at 4 °C. After washing with PBS, labeling was visualized with fluorescence-labeled secondary antibodies (DAKO).

PC12 cells and primary neurons were fixed in increasing concentrations (0.4–4%) of *para*-formaldehyde, washed in PBS, and mounted in Crystal/mount (Biomeda, Foster City, CA). In some experiments, EGFP signals were enhanced with Ab6556 (Abcam, Cambridge, UK), which was applied at a dilution of 1:500–1:1000 in 2% bovine serum albumin, 2% goat normal serum in PBS. Signal specificity was fully confirmed using $Ab^{420-430}$. Counter staining was routinely done with 0.05% rhodamine phalloidin (Molecular Probes) or with antibodies to α-actinin or synapsin I at a dilution of 1:500. Cells were examined on an epifluorescence microscope with digital image capturing (AxioVision 4, Zeiss).

Expression Systems and Site-directed Mutagenesis—Fusion proteins of Ndr2 and the enhanced green fluorescent protein (EGFP) were generated using vector pEGFP-c1 (BD Biosciences) and the amplified *Ndr2* coding region (see MBP::Ndr2 fusion). Ser^{282}-Ala/Thr^{442}-Ala double mutants of EGFP::Ndr2 were generated using a site-directed mutagenesis system (QuikChange, Stratagene), according to the manufacturer's instructions. Primers 5′-GGAGACAGCTGGCTTAC (T → G) CCACAG TTGGAACACCAGAC-3′ (for Ser^{282}) and 5′-GACTGGGTTTTTCTCAA-TTAC (A → G) CCTACAAAAGGTTTGAAGGG-3′ (for Thr^{442}) and the corresponding reverse primers were used to introduce the indicated point mutations, which were subsequently combined using an in-between AccI restriction site.

Cell Culture PC12—Rat pheochromocytoma (PC12) cells were cultured in 85% RPMI 1640 with 2 mM L-glutamine, 10% horse serum, and 5% fetal bovine serum (all reagents from Invitrogen, Eggenstein, Germany). Transfections with plasmids expressing native EGFP::Ndr2, mutant EGFP::Ndr2, or EGFP were performed using the GeneJammer reagent (Stratagene). Stable transfected cells were selected with 500 μg/ml G418 (Invitrogen) and maintained under 200–400 μg/ml of G418 during neurite outgrowth experiments. For assessment of neurite outgrowth and intracellular localization of Ndr2, acute and stable cells were allowed to adhere to poly-D-lysine-coated coverslips and cultured in 97% RPMI 1640 with 2 mM L-glutamine, 2% horse serum, and 1% fetal bovine serum. A putative association of EGFP::Ndr2 with the actin cytoskeleton or microtubules was addressed through treatment of stably transfected cells for 3 h with 10 μM latrunculin B (Molecular Probes) or 100 μM colchicine (Sigma), respectively. PC12 neurite outgrowth was determined with and without supplementation of nerve growth factor (NGF, 50 ng/ml, New England Biolabs) for up to 5 days. The proportion of transfected cells producing neurites of >10 μm was determined at different time points after seeding. For a detailed analysis of neurite extension and branching, 5% of transfected cells with the largest neurites in each sample were reconstructed (Neurolucida, Microbrightfield, Magdeburg, Germany) and compared between groups. In addition, phospho-serine immunoblot analyses were performed in early outgrowing cultures. Each 2×10^5 cells per line were collected during the first day of neurite outgrowth culture and treated with a boiling buffer containing 125 mM Tris, pH 6.8, 4% SDS, 20% glycerol, 10% β-mercaptoethanol for 5 min. Proteins were separated on 8% SDS-PAGE and analyzed in immunoblots with antibodies directed against phosphoserine and β-actin. Statistical comparisons were done with Student's unpaired *t* test and the Mann-Whitney *U* test.

Cell Culture of Primary Neurons—Primary cortical neurons were obtained from day 19 embryonic Long Evans rats (modified from Ref. 15). In brief, after treatment with 0.5% trypsin in Hanks' buffered salt solution (Invitrogen) and 0.01% of DNase I, cells were dissociated mechanically using a Nylon mesh (aperture, 125 μm) and suspended in Dulbecco's modified Eagle's medium (Invitrogen). 40,000 cells each were plated on poly-D-lysine-coated coverslips and grown for 14 days before transfection with 2 μg of plasmid DNA in 72.5 μl of a buffer containing 42 mM Hepes, 74 mM NaCl, 10 mM KCl, 1.4 mM Na_2HPO_4, 15 mM glucose, and 125 mM $CaCl_2$ together with 10 μl of Neurobasal medium (Invitrogen) and 2.5 μl of NeuroPORTER (Gene Therapy Systems, Inc., San Diego, CA) at pH 7.05. Cultures were examined with an epifluorescence microscope 48 h after transfection.

RESULTS

Isolation and Differential Expression of Ndr2—The 200-bp clone #VIIE6 (Fig. 1*A*) was selected from a group of 21 gene products that were differentially expressed in the amygdala during consolidation of fear memory (2). As the first step in our analysis, the induction of Ndr2 expression was confirmed with PCR-based Northern analysis on amygdala samples pooled from each group of four animals (2) (Fig. 1*B*). A double band at 3.0/2.8 kb could be detected with probe #VIIE6 and later with probes generated from the 5′-RACE product. Overexposure of blots revealed an additional hybridization signal at ~4.5 kb (data not shown), which corresponds to the length of the sequenced *Ndr2* (*Stk38l*) mRNA and the size of *Ndr2* detected on standard Northern blots (Fig. 1*C*). Quantitative analysis of *Ndr2* transcript levels at the major double band revealed an increase in fear-conditioned animals 6 h after training (181.4 ± 24.2% of control levels, $p < 0.05$, Student's *t* test, $n = 4$ independent behavioral experiments). A similar increase was also observed for the 4.5-kb signal, although reliable quantification was not possible in the overexposed blots. The pseudo-conditioned group showed a partial increase of expression (139.9 ± 10.9% of control levels, $p < 0.05$). At a later time point, 24 h after training, no difference of *Ndr2* expression could be observed in either experimental group compared with the unconditioned control animals (fear-conditioned: 106 ± 27.8%, pseudo-conditioned: 108 ± 20.9% of control levels; $n = 3$).

Differential expression of Ndr2 after fear conditioning was confirmed on individual animals in an independent behavioral experiment (Fig. 1*D*). The analysis with real-time PCR of Ndr2 expression levels in four different brain areas showed specific increases in the basolateral complex of the amygdala for both fear-conditioned (245.4 ± 125.6% of control levels, $p < 0.05$, $n = 5$) and pseudo-conditioned mice (710.0 ± 307.1% of control levels, $p < 0.01$, $n = 5$). Moderate increases were also observed in frontal cortical samples (fear-conditioned mice: 209.9 ± 114.3% of control levels) and in the hippocampus of pseudo-conditioned animals (194.4 ± 93.4% of control levels). These, however, failed to reach significance level. No difference was observed between groups in the cerebellar cortex (fear-conditioned, 116.4 ± 43.2%; pseudo-conditioned, 91.4 ± 27.1%).

Sequence of Ndr2—With 3′-RACE and 5′-RACE we isolated 4557 bp of Ndr2 (Stk38l) mRNA that cover the entire coding sequence and 3′-untranslated region (sequence information was deposited with GenBank™ accession number AY223819). Clone #VIIE6 of the subtracted library located to bp 3742–3941 of this sequence (Fig. 1*A*). A Kozak consensus sequence and translation start was found in the 5′-RACE product, followed by an open reading frame of 1368 bp. The coding region and following 900-bp are identical to the recently identified mNdr2 clone (AY292400 (12)). However, 5′- and 3′-untranslated regions of these sequences differ in that we isolated a 40-bp 5′ region that was not found in the clone described by Stegert and co-workers, and an additional 2.3-kb 3′-untranslated region following the first putative polyadenylation signal. Northern analysis and a vast majority of expressed sequence tag hits in GenBank™ indicate that our clone resembles the predominantly expressed Ndr2 transcript.

Gene Location and Gene Structure—Radiation hybrid mapping and GenBank™ analysis located the *Ndr2* gene to mouse chromosome 6, 9.65 centi Ray from D6Mit294 (logarithm of odds score > 3.0). This could be confirmed by an NCBI GenBank™ search that further suggested that human *NDR2* locates to chromosome 12 p11. The mouse gene comprises 14 exons, which span a total of 54 kb, with a first intron of 33 kb in length. In the putative promoter region, two SP1 elements could be identified at positions −155 and −10, a serum-responsive element at position −30, and a cyclic AMP-responsive element (CRE) consensus site at position −89 toward a twin GC box. Various potential polyadenylation sites were identified between positions 2256 and 4517, but Northern blot analysis illustrated the preferential expression of an *Ndr2* mRNA species with a length of 4.5 kb in various tissues (see Fig. 1*C*). The

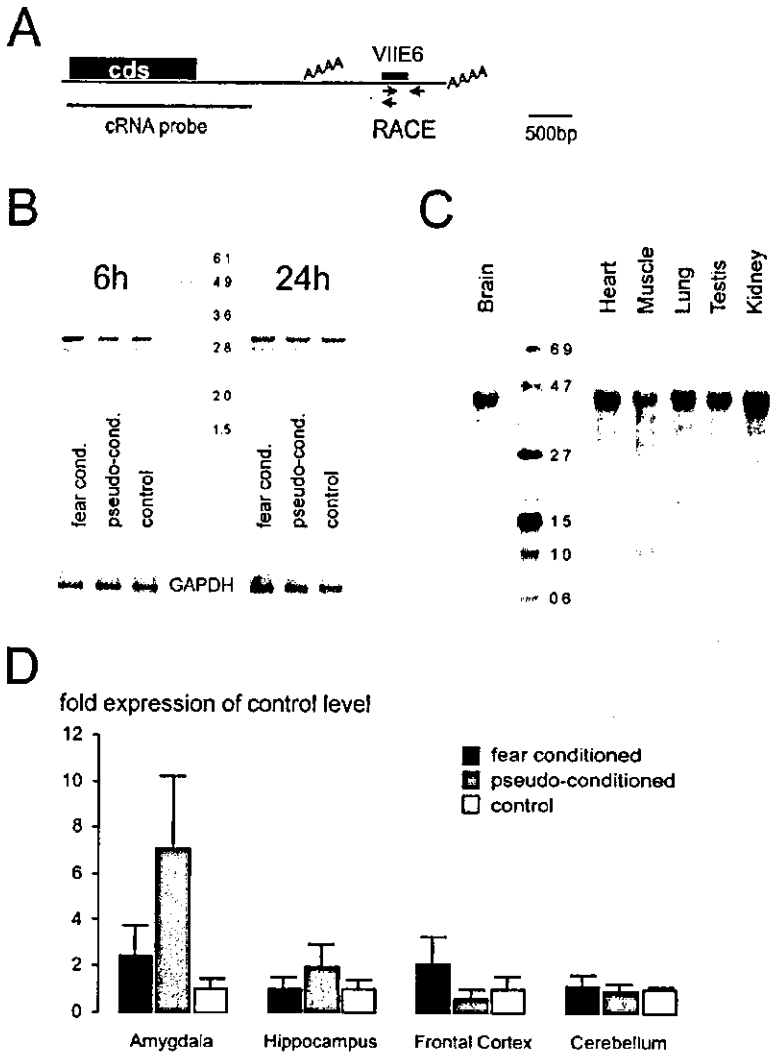

FIG. 1. ***Ndr2* mRNA, schematic drawing, and expression.** *A*, starting from clone #VIIE6, *Ndr2* full-length mRNA was obtained with 3′-RACE and nested 5′-RACE using primers at the location indicated (*arrows*). The indicated cRNA probe was used for both Northern analysis and *in situ* hybridization. *cds*, coding sequence. *B*, increased expression of *Ndr2* mRNA in the basolateral complex of the amygdala after fear conditioning training, illustrated by blot analysis of amygdala RT-PCR products. *Ndr2*-labeled double bands with a size of ~3.0 kb and 2.8 kb; such double banding and size shift are frequently observed and likely due to premature incorporation of the 5′ extension oligonucleotide. A similar change is evident for a 4.5-kb signal after overexposure (not shown), but no difference can be observed at a later time point, 24 h after training. *C*, Northern analysis revealed widespread expression of *Ndr2* mRNA in all tissues analyzed. A 4.5-kb transcript was detected that corresponds to the predicted size of the full-length *Ndr2*. *D*, relative *Ndr2* expression in different brain areas after fear conditioning, determined by real-time PCR (mean ± S.D., $n = 5$). Significant increases were observed in the amygdala of both fear-conditioned and pseudo-conditioned animals, compared with unconditioned controls. Moderate increases in the frontal cortex and in the hippocampus of pseudo-conditioned mice were also observed. The cerebellar cortex, which is not critically involved in Pavlovian fear conditioning, showed no change *of Ndr2* expression.

smaller size of fragments in PCR-blot analysis thus is likely a result of premature incorporation of the 5′-oligonucleotide and preferential amplification of small PCR products.

Ndr2 Expression in the Brain—In situ hybridization revealed a widespread expression of *Ndr2* at moderate levels throughout the brain (Fig. 2). The highest staining intensity was observed in the neocortex, basal forebrain, hippocampus (particularly area CA3), the amygdala, cerebellum, and several brainstem nuclei. The results were corroborated by immunohistochemical staining using $Ab^{420-430}$, which was abolished after preincubation of antibodies with immunization peptide or bacterially expressed Ndr2 protein (data not shown). In the hippocampus putative interneurons of stratum oriens and stratum radiatum, as well as the hilus were strongly labeled. Within the amygdala, a large number of pyramidal-shaped class I neurons was stained. No changes in the labeling intensity or distribution of Ndr2-expressing cells could be observed after fear conditioning by either *in situ* hybridization or immunohistochemistry.

At higher magnification, the immunohistochemical staining suggested a punctuate distribution of Ndr2 immunoreactivity within the labeled cells (Fig. 2, *K* and *L*). Some actions of Ndr family kinases appear to involve regulation of transcriptional processes, and a conserved atypical nuclear location sequence can indeed be found in Ndr2. However, we did not find evidence for a nuclear localization of Ndr2 in the amygdala of fear-conditioned or control animals. Instead, staining was observed in the cytosol near the cell surface and in the surrounding neuropil.

Intracellular Localization of Ndr2—We therefore further investigated the intracellular distribution of EGFP::Ndr2 fusion protein in stable (Fig. 3, *A–H*) or acutely transfected PC12 cells (Fig. 3*I*) and in acutely isolated cortical neurons (Fig. 3, *J–L*). In all experiments, EGFP::Ndr2 located to somata and neurites, but no or only weak labeling was observed in the nucleus. This is in contrast to control cells, which showed a predominant nuclear localization of EGFP (Fig. 3*F*). Cytoplasmic EGFP::Ndr2 often had a filamentous appearance with a high density in the perinuclear cytoplasm, closely resembling the pattern of stress fibers (Fig. 3*A*, but see also the granular staining in Fig. 3*I*). Double labeling with phalloidin-rhodamine indeed suggested a co-localization of Ndr2 with actin filaments in the cytoplasm of PC12 cells and cortical neurons. Intensive double labeling was also frequently observed at sites of cell-cell contact (Fig. 3*B*), but α-actinin-positive focal adhesions were devoid of EGFP::Ndr2 (Fig. 3*C*). Ndr2 was further observed in growth cones and pre-synaptic sites (Fig. 3, *D* and *E*). High resolution images showed EGFP::Ndr2 localization in filopodia extending from the soma or the growth cone, often beyond the extension of the phalloidin staining (Fig. 3*D*). In acutely transfected cells with a high expression of EGFP::Ndr2 and to lesser extend in some stably transfected cells, a granular staining pattern could be observed in addition to the filamentous labeling in F-actin-rich

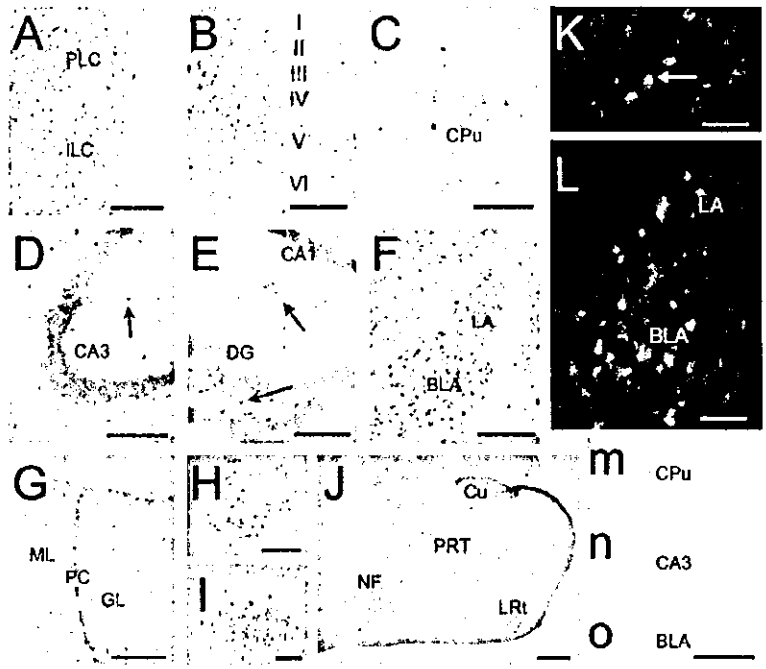

FIG. 2. **Colorimetric *in situ* hybridization (*A–J*) and fluorescence immunohistochemistry (*K* and *L*) show Ndr2 expression in the mouse brain.** *A*, a coronal section showing considerable *Ndr2* expression in frontal cortical areas. *PLC*, prelimbic cortex. *ILC*, infralimbic cortex. *B*, less intense labeling was observed in the parietal cortex, but *Ndr2*-positive cells were found throughout layers II-VI. *C*, in the caudate putamen (*CPu*) pronounced labeling of few single neurons could be observed. *D*, hippocampal area CA3. Pyramidal cells and interneurons in the stratum oriens and (*arrow*) stratum radiatum showed intense labeling. *E*, similar intense staining was observed for interneurons in area CA1 and the hilus (*arrows*), whereas CA1 pyramidal cells and granule cells of the dentate gyrus were only moderately positive for *Ndr2*. *F*, coronal section through the amygdala demonstrating strong *Ndr2* expression in the basolateral and, less prominently, in the lateral amygala. No discernable change of Ndr2 expression and distribution was seen in the same area of fear-conditioned or pseudo-conditioned animals (data not shown). *LA*, lateral amygala. *BLA*, basolateral amygdala. *G*, in sections through the cerebellar cortex, a prominent labeling of Purkinje cells was observed. Positive cells were also found in the molecular and granule cell layer. *GL*, granule cell layer; *PC*, Purkinje cell layer; *ML*, molecular layer. *H*, a subpopulation of projection neurons in deep cerebellar nuclei were also clearly positive for *Ndr2*. *I*, intense labeling was further seen in the facial nucleus and other brainstem areas overviewed in *J*. *NF*, nucleus facialis; *PRT*, parvocellular reticular nucleus; *CU*, cuneate nucleus; *LRt*, lateral reticular nucleus. *K*, immunohistochemistry with $Ab^{420-430}$ revealed intensively labeled neurons in the hilus. Cellular labeling was not homogeneous, but patches of intense labeling are apparent close to the cell membrane (*arrow*). *L*, in the LA and BLA, several Ndr2-immunoreactive cells could be identified. According to their size and shape these appear to be class I pyramidal cell-like neurons, which comprise the major population of projection neurons in these amygdala subnuclei. *Small lettering*: sense controls in the caudate putamen (*m*), the CA3 region of the hippocampus (*n*), and the basolateral amygdala (*o*). *Bars*, 500 μm in *J*, 100 μm in *K* and *L*, and 200 μm elsewhere.

regions (Fig. 3, *E* and *I*). Cortical neurons showed pronounced labeling of somata and dendrites, as well as dendritic spines (Fig. 3, *J* and *K*); labeling of outgrowing axons was also observed (Fig. 3*L*). Mutant EGFP::Ndr2 showed an identical intracellular distribution (data not shown). To confirm the putative association of EGFP::Ndr2 with the actin cytoskeleton, we disrupted actin filaments in PC12 cells with a moderate latrunculin B treatment, which left neurites and cell structure largely intact. This treatment led to a striking re-distribution of EGFP::Ndr2 and its accumulation in the nucleus, thus closely resembling the staining pattern of EGFP itself (Fig. 3*G*). Remainders of the somatic actin cytoskeleton were only faintly labeled. Treatment with colchicine, which led to an entire disintegration of neurites, did not affect the localization of Ndr2 fusion protein in the soma nor in filopodia of somatic origin (Fig. 3*H*).

Interaction with Actin—Purified MBP::Ndr2 and $Ab^{420-430}$ were used for the analysis of a putative interaction with actin or actin filaments in pull-down and co-precipitation assays. In fact, it was possible to precipitate β-actin from crude brain protein extracts with bacterially expressed MBP::Ndr2 fusion protein, but not with MBP itself (Fig. 4*B*). A cleavage of MBP::Ndr2 with factor X before incubation prevented this precipitation of β-actin (not shown). Other cytoskeletal and cytoskeleton-associated proteins such as β-tubulin and neurofilament proteins (Fig. 4*B*), α-actinin, synapsin I, kinesin light and heavy chains, β/δ-catenin, and β-spectrin, could not be detected after precipitation. Experiments with $Ab^{420-430}$ supported these findings in that β-actin was co-precipitated with Ndr2 from crude PC12 cell protein extracts (Fig. 4*C*). Interestingly, the β-actin precipitate was highly immunoreactive for phospho-serine.

Cellular Functions of Ndr2—Next, we addressed possible cellular functions of Ndr2 in PC12 cells as a model system for cellular differentiation and neurite outgrowth. Overexpression of EGFP::Ndr2 resulted in an increased growth of neurites in the absence of NGF and a reduced spreading of cells on the substrate (Fig. 5).

Proliferation—During preparation of the experiments with stably transfected cells we observed that both lines of *EGFP::Ndr2*-transfected cells (average duplication times of 34.9 and 32.7 h), but not *EGFP*-transfected cells (44.9 h) or mutant controls (47.7 h) showed a higher proliferation rate than non-transfected PC12 cells (46.2 h) when grown in suspension. As a general rule, EGFP::Ndr2-expressing cells grew in large, floating clusters of cells and failed to form stable monolayers on the plastic surface as seen in control groups.

Cell Spreading—In adherent cultures, we observed striking differences in cellular morphology between cell lines (Fig. 5, *A* and *C*). Under treatment with NGF, cells of all lines showed an increased adhesion and spreading on the substrate. However, the percentage of such spreading cells was significantly reduced in *EGFP::Ndr2*-transfected cells compared with *EGFP*-transfected controls (without NGF: *EGFP::Ndr2* 9.2 ± 3.8%

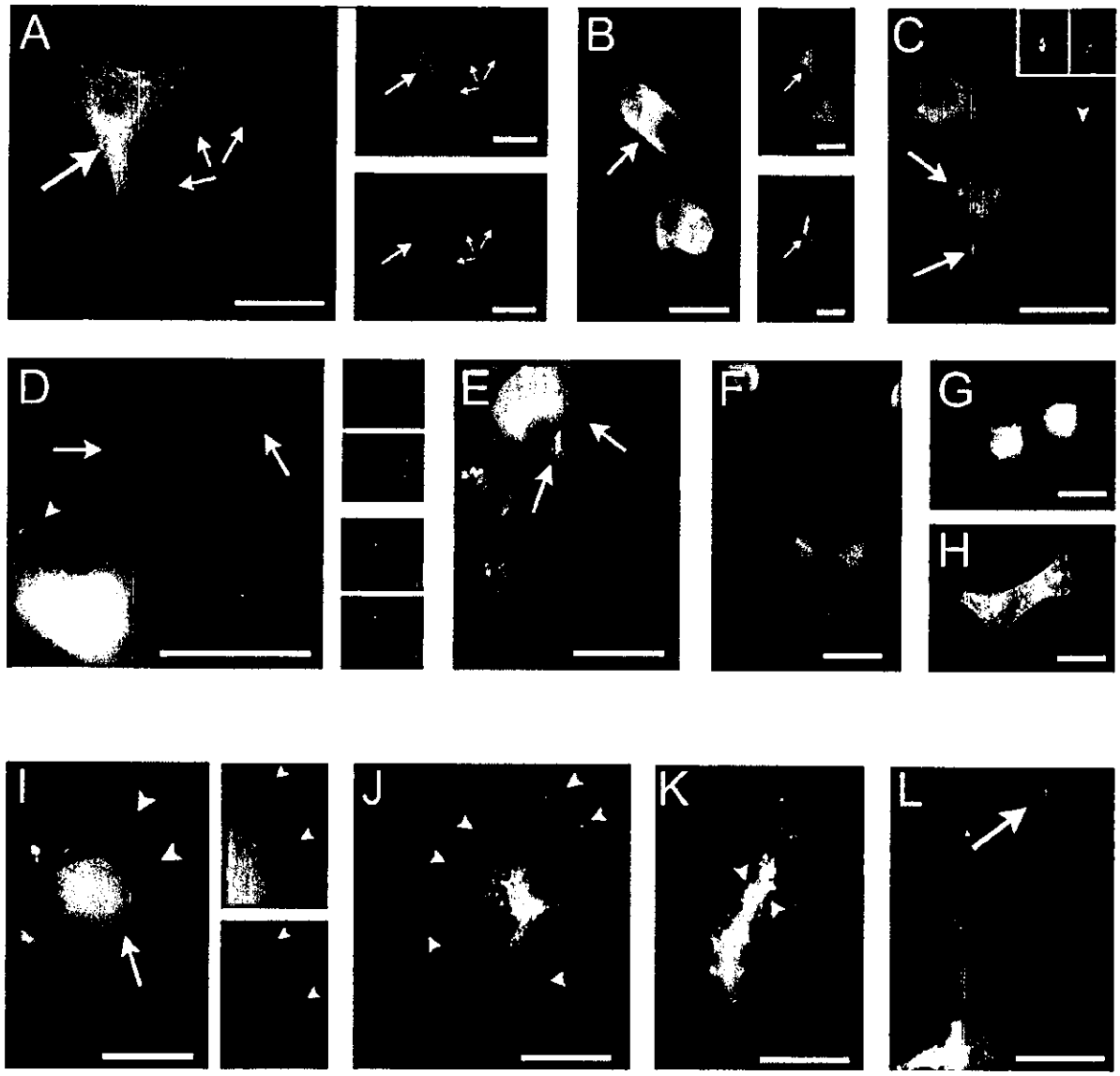

FIG. 3. **Distribution of EGFP::Ndr2 fusion protein (*green*) in transfected PC12 cells (*A–I*) and acutely isolated cortical neurons (*J–L*).** Counterstaining was done with rhodamine-phalloidin (*red*) as indicator of actin filaments, unless indicated otherwise. *A*, shows the network-like distribution of EGFP::Ndr2 in the soma and its co-localization with actin filaments. Their concentration at the perinuclear space (*large arrow*) and the pronounced double labeling of somatic filopodia (*small arrows*) are indicated. *B*, EGFP::Ndr2 was found enriched and co-localizing with actin fibers at some sites of cell-contact (*arrows*), in particular in groups of largely undifferentiated cells. *C*, counterstaining with α-actinin indicates co-localization at sites of beginning neurite outgrowth (*arrowheads, single color insets*), but apparent absence of EGFP::Ndr2 from focal adhesion sites (*arrow*). *D*, growth cones (*arrows, single color images*) and membrane ruffles (*arrowheads*) were frequently double labeled with EGFP::Ndr2 and rhodamine-phalloidin. *E*, shows two pre-synaptic sites (*arrows*), double labeled for EGFP::Ndr2 and α-actinin. Note the granule-like labeling pattern in these cells. *F*, controls showed a predominantly nuclear localization of EGFP. *G*, after disruption of actin filaments with latrunculin B, EGFP::Ndr2 accumulated in the nucleus, reflecting the expression pattern of EGFP in controls. *H*, colchicine treatment did not affect the somatic distribution of EGFP::Ndr2. *I*, distribution of EGFP::Ndr2 in an acutely transfected PC12 cell. In addition to its co-localization with actin filaments (*arrowheads, single color images*) Ndr2 was found in granules (*arrow*) dispersed over the cytoplasm. Although filamentous labeling was apparent in all cells, the number of granules appeared to vary with EGFP::Ndr2 expression level. *J* and *K*, somatic and dendritic distribution of EGFP::Ndr2 in a transfected cortical neuron. *Arrowheads* indicate co-localization with actin filaments at positive post-synaptic sites (spines). *L*, localization of Ndr2 in an outgrowing axon (*arrow*). *Bars*, 20 μm.

and 11.6 ± 2.0%, *EGFP* 17.8 ± 4.4%, $p < 0.01$; with NGF: *EGFP::Ndr2* line 1 10.4 ± 0.9%, *EGFP* 50.1 ± 4.6%, $p < 0.01$). Double mutation of Ser^{282} and Thr^{442} reduced the effects of EGFP::Ndr2 expression (without NGF: 15.9 ± 6.7%; with NGF: 36.0 ± 11.1%).

Neurite Outgrowth—In the absence of NGF, cells of all lines developed short and simple, but clearly discernable neuritic processes. However, the percentage of cells that produced such short neurites in *EGFP::Ndr2*-transfected cells (74.6 ± 8.3%) were significantly higher than in *EGFP*-transfected controls (56.8 ± 6.5%; $p < 0.01$). The difference was particularly evident when only cells with neurites >10 μM were considered (36.3 ± 10.9% *versus* 6.6 ± 1.5%; $p < 0.01$) (Fig. 5, *A* and *B*). Increased neurite outgrowth was also observed in a second line of *EGFP::Ndr2*-transfected cells (68.1 ± 3.7% total and 10.6 ± 2.8% >10 μM; $p < 0.05$), but was abolished after double mutation of the activation sites Ser^{282} and Thr^{442} (54.9 ± 6.3% total and 7.6 ± 2.6% >10 μM). On the contrary, following NGF treatment a slight non-significant reduction in the number of cells that developed discernable neurites was apparent in

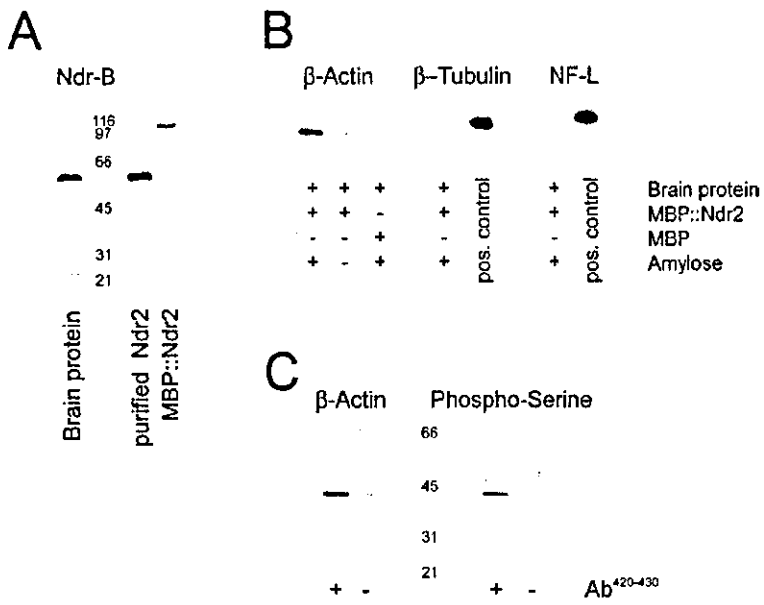

FIG. 4. **Ndr2 protein and precipitation of actin.** (A) Ndr2 was detected in 100 μg of total brain homogenate using $Ab^{420-430}$. In addition to a signal at the predicted molecular mass of 54kD, background staining of several high and low molecular weight proteins was seen in all SDS-PAGE preparations. The lanes on the right show purified Ndr2 protein from the brain and bacterial MBP::Ndr2 fusion protein. (B) Pull down assays with MBP::Ndr2 fusion proteins precipitated β-actin from brain protein extracts. Only traces of β-actin were seen in MBP precipitates or after omission of amylose. In contrast, we entirely failed to detect β-tubulin or neurofilament proteins in MBP::Ndr2 precipitates. For both, crude brain protein extracts served as positive controls. *NF-L*, neurofilament light chain. *C*, β-actin was also co-precipitated with Ndr2 through $Ab^{420-430}$, whereas only background actin labeling was observed when the primary antibody was omitted. Analysis of precipitates with phospho-serine antibodies further suggests that a considerable proportion of the precipitated β-actin was phosphorylated.

EGFP::Ndr2-transfected cells (78.1 ± 22.1%) compared with *EGFP* controls (91.0 ± 5.4%). Ser^{282}/Thr^{442} double mutants showed intermediate values (82.9 ± 4.5%). The length of neurites (mean ± S.D. of cells with total neurite length of >100 μm: *EGFP::Ndr2* 216.7 ± 64.6 μm, control *EGFP* 222.4 ± 84.6 μm) and their branching pattern (*i.e.* frequency of first, second, and third order branches) did not differ. To address putative mechanisms of Ndr2 function, we determined protein serine phosphorylation in PC12 cells on the first day of neurite outgrowth, *i.e.* before their development of significant differences in neurite length. In our immunoblot analyses we could distinguish at least eight major phospho-serine protein bands, two of which with molecular weights of 36 and 42 kDa showed a higher degree of serine phosphorylation in Ndr2-expressing cultures than in EGFP and mutant Ndr2 controls (Fig. 5*D*). Quantification in triplicate experiments showed an increase of the 42-kDa band to 218.7 ± 45.1% of baseline values (*i.e.* in floating cells) in *EGFP::Ndr2*-transfected cells, but no change from baseline in phosphorylation of EGFP or Ser^{282}/Thr^{442} mutant controls (96.0 ± 10.6% and 82.9 ± 18.7%, respectively; between group comparison: $p < 0.05$). A similar, but not statistically significant change was observed for the 36-kDa signal (EGFP::Ndr2: 273.6 ± 151.5%, EGFP controls: 93.9 ± 50.9% mutant controls: 57.4 ± 19.6%). Furthermore, a reduced phosphorylation of a double band at ~100 kDa was observed independently of neurite outgrowth in *EGFP::Ndr2*-transfected cells (49.3 ± 17.3% of control cell levels; $p < 0.05$), but not in Ser^{282}/Thr^{442} mutant controls (100.2 ± 28.1% of control cell levels).

Acute Transfection—Acute EGFP::Ndr2-transfected cells also showed a greatly reduced adhesion and spreading on the substrate (4.8 ± 3.0% with NGF, 3.3 ± 3.3% without NGF), compared with cells transfected with EGFP (35.5 ± 8.3% with NGF, 16.7 ± 8.6% without NGF, $p < 0.01$ for both). In fact, cells with the highest expression of EGFP::Ndr2 did not even attach to the dish in these experiments. Mutated EGFP::Ndr2 had no such effect (27.2 ± 6.0% with NGF, 15.5 ± 5.0% without NGF). At the same time we observed a reduction of neurite outgrowth ($p < 0.01$) in acutely EGFP::Ndr2-transfected cells (7.1 ± 7.0% with NGF, 3.3 ± 3.3% without NGF) compared with EGFP (55.4 ± 7.0% with NGF, 23.8 ± 9.9% without NGF, $p < 0.01$ for both), contrasting the enhancement of neurite outgrowth in stably transfected cell lines. Mutated EGFP::Ndr2 showed intermediate effects depending on the stimulation with NGF (35.1 ± 9.0% with NGF, $p < 0.01$; 6.7 ± 5.1% without NGF, not significant).

DISCUSSION

To address the cellular and molecular processes that underlie memory consolidation and neural plasticity, we study gene products that are expressed in the mouse amygdala after classic fear conditioning (2). Here we describe the cloning and functional characterization of a novel serine/threonine kinase expressed in the brain, Ndr2 (Stk38l), the expression of which is transiently increased in the amygdala during the consolidation of Pavlovian fear memory. Our experiments provide evidence for an interaction of Ndr2 with the actin cytoskeleton and its putative involvement in control of cell morphology and differentiation in neuronal and neuronal-like cells.

A fragment of the *Ndr2* 3′-untranslated region was obtained through subtractive hybridization cloning from the amygdala of fear-conditioned mice (2). PCR-based gene expression analysis confirmed that *Ndr2* transcript levels were transiently elevated in the amygdala of fear-conditioned and pseudo-conditioned animals 6 h after training and returned to baseline within 24 h. Thus, during consolidation of fear memory, *Ndr2* mRNA levels are regulated in the basolateral complex of the amygdala in a learning- and stress-dependent manner, similar to several other signal transduction and structural re-organization factors (2). GenBank™ analysis suggests that transcription of the *Ndr2* gene may be driven through cyclic AMP response elements (CRE) or serum-responsive elements. These are potential targets for the CRE-binding protein CREB and the mitogen-activated protein kinase pathway in amygdala neurons, respectively, which may explain the observed induction of gene expression after fear conditioning training.

Moderate induction of *Ndr2* in two other areas concerned with fear memory, the frontal cortex, and the hippocampus (after pseudo-conditioning), indicates a more general role in information storage in the fear-conditioning circuits and should prompt further investigation. For example, a tendency for increased *Ndr2* expression in the hippocampus of pseudo-conditioned animals may relate to a preferential storage of contextual information in this training group. Due to a considerable baseline expression and apparently distributed induction after fear conditioning, changes in the expression of Ndr2 could not

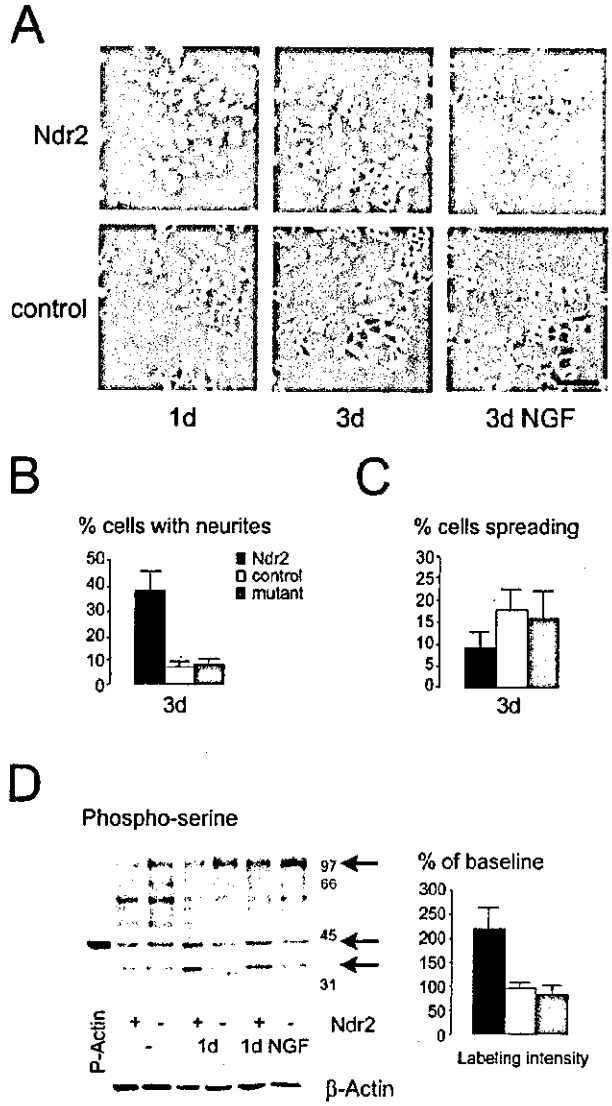

FIG. 5. **Ndr2 facilitates neurite outgrowth in the absence of NGF and reduces cell spreading on the substrate.** *Photographs* in *A* show representative examples of EGFP::Ndr2-transfected cells and EGFP-transfected control cells, grown for 1 day (*1d*) or 3 days (*3d*) in the absence, or for 3 days in the presence of NGF (*3d NGF*). The *graphs* summarize the difference between experimental groups in neurite outgrowth (*B*) and cell spreading (*C*; $n = 6$). Increased neurite growth was particularly evident on day 3 without NGF treatment. On the other hand, a reduction of cell spreading was seen both in the presence and absence of NGF. Both effects were abolished in cells expressing mutated Ndr2. *D*, increased protein serine phosphorylation was evident during neurite outgrowth in cells transfected with EGFP::Ndr2. *Arrows* indicate two proteins with molecular masses of ~36 and 42 kDa that showed consistently increased phosphorylation and a double band at ~100 kDa with reduced phosphorylation compared with controls. The *graph* presents the increase of β-actin phosphorylation in different lines, compared with baseline levels (mean ± S.E., $n = 3$).

be visualized by *in situ* hybridization or immunohistochemistry. In fact, expression of Ndr2 was also observed in various cortical and subcortical brain areas that do not relate to the fear conditioning circuitry (Fig. 2).

Ndr1 and Ndr2 belong to a family of growth-related protein kinases, which are involved in proliferation and cellular differentiation in yeast, *Caenorhabditis elegans*, *Drosophila melanogaster*, and mammals (11). Several lines of evidence indicate that molecular processes of growth and structural re-organization indeed occur in the mammalian amygdala during consolidation of fear memory (16). In particular, these may involve modifications at the actin cytoskeleton, which are critical for neural plasticity and memory formation (9). Previous observations of a differential expression of actin isoforms (2) and the activation of $p160^{ROCK}$ (8) in the amygdala during or following fear conditioning support this view. Findings in other organisms indicate that Ndr kinases may be involved in pathways that control such actin filament dynamics: the Ndr kinase orthologue in *D. melanogaster*, *Triconcerned*, interacts with the actin cytoskeleton and co-ordinates growth of actin filaments (17), and the Ndr kinase orthologue in *C. elegans*, SAX-1, shares function with the RhoA-GTPase signaling pathway during neurite formation (18). We, therefore, focused our analysis of Ndr2 function on a potential association with the actin cytoskeleton and on actin-mediated functions in a cellular model of neuronal differentiation.

As a first step, we determined the intracellular localization of EGFP::Ndr2 fusion proteins in differentiated PC12 cells and acutely isolated cortical neurons. We could show that EGFP::Ndr2 co-localizes with actin filaments at the somata, at some sites of cell contact including synapses, at the growth cones and filopodia of PC12 cells, as well as in dendrites, spines, and outgrowing axons of cortical neurons. This labeling pattern matches the distribution of Ndr2 immunohistochemical preparations from the brain and was sensitive to disruption of actin filaments with latrunculin B. Data from our immunoprecipitation and pull-down experiments indicate that Ndr2 is indeed able to bind (phospho-) actin. Interestingly, highly overexpressing cells showed an accumulation of EGFP::Ndr2 in granule-like structures similar to those reported recently by Devroe and co-workers (13), in addition to actin filaments. The composition of these granular structures and the mechanisms of Ndr2 association with different intracellular compartments remain to be investigated.

In the course of our localization experiments we also obtained evidence for an involvement of Ndr2 in actin-mediated cellular functions, in that cells expressing EGFP::Ndr2 displayed consistently reduced spreading on the substrate. Spreading of PC12 cells, *e.g.* after RhoA activation, is typically accompanied by the formation of focal adhesions and stress fibers (19). However, focal adhesions generally were devoid of EGFP::Ndr2 in our experiments. This exclusion from stabilized contact sites and the reduced spreading suggest that Ndr2 may negatively regulate substrate adhesion in differentiated PC12 cells, possibly by reducing the stability of actin-dependent contact sites. Reduced PC12 cell adhesion, by virtue of a reduced contact inhibition, may also explain the increased proliferation of these cells (20) in line with the observation that inhibition of the potential Ndr-kinase activator S100B (21) both induces flattening of glia cells and reduces their proliferation (22).

Some S100 proteins are also potent inducers of neurite outgrowth (23). In fact, we found that EGFP::Ndr2 in stably transfected cell lines facilitated the formation of short neuritic processes in the absence of NGF, although it did not enhance NGF-induced outgrowth nor affect the length or complexity of neuritic trees in NGF-treated cells. Acutely transfected cells on the contrary showed reduced neurite outgrowth both in the presence and absence of NGF.

We believe that facilitation of neurite outgrowth through Ndr2 is limited by the simultaneous reduction of matrix adhesion, and that high expression levels after acute transfection precluded neurite outgrowth in our experiments. This can be explained with an enhancement of actin dynamics through Ndr2 resulting in competing cellular effects. The kinase appears to be well suited to translate Ca^{2+} signals, which are critical for both NGF-dependent and NGF-independent neurite

outgrowth, to the actin cytoskeleton (12). In fact, several conserved regulatory amino acid motifs indicate that the Ndr2 protein is a site of convergence for Ca^{2+}/S100, protein kinase A, and mitogen-activated protein kinase signaling pathways, all of which are involved in neurite outgrowth in PC12 cells (22–25), as well as amygdalar processes during fear memory consolidation (reviewed in Ref. 4).

In support of this view we finally found that the facilitatory effect of Ndr2 on NGF-independent neurite outgrowth was preceded by increases of phosphorylation in at least two proteins, one of which co-migrated with β-actin. We are currently identifying hyperphosphorylated proteins in Ndr2-expressing cells and investigating their role in Ndr2-induced neurite outgrowth. So far we could show that Ndr2-mediated cellular effects are dependent on its kinase activity: double mutation of the activity-controlling phosphorylation sites at Ser^{282} and at Thr^{442} (12) counteracted the Ndr2-induced reduction of cell spreading and changes in neurite outgrowth, as well as associated changes in protein phosphorylation. Protein kinases and phosphatases play key roles in cytoskeleton re-arrangement during cellular growth and differentiation. For example, phosphorylation through protein kinase A has been shown to stabilize actin monomers and to prevent filament formation, whereas protein kinase C increases the incorporation of actin into filaments (26, 27). Our data indicate that Ndr2 by controlling actin phosphorylation and actin filament dynamics may play an important role in cell adhesion and neurite outgrowth.

Several molecular and cellular processes have been identified that are involved in increased activity and synchronization of projection neurons in the lateral amygdala after fear conditioning (4). Other molecular changes provide evidence for learning-related structural plasticity in the amygdala (16). However, memory-related synaptogenesis or changes in spine density like in the hippocampus (28, 29) have not yet been demonstrated in the amygdala. Its widespread expression in the brain, the learning-coordinated induction in the amygdala, and its molecular characteristics make Ndr2 a highly interesting molecular target for the analysis of actin-mediated cellular processes related to morphological re-organization and fear memory consolidation.

Acknowledgments—We thank Margit Schmidt, Sandra Vorwerk, and Simone Stork for expert technical assistance and are grateful to Dr. Thomas Dresbach and Dr. Peter Landgraf for help with cell culture experiments.

REFERENCES

1. Kandel, E. R. (2001) *Science* **294,** 1030–1038
2. Stork, O., Stork, S., Pape, H.-C., and Obata, K. (2001) *Learn. Mem.* **8,** 209–219
3. LeDoux, J. E. (2000) *Annu. Rev. Neurosci.* **23,** 155–184
4. Stork, O., and Pape, H.-C. (2002) *Cell Tissue Res.* **310,** 271–277
5. Schafe, G. E., Atkins, C. M., Swank, M. W., Bauer, E. P., Sweatt, J. D., and LeDoux, J. E. (2000) *J. Neurosci.* **20,** 8177–8187
6. Schafe, G. E., and LeDoux, J. E. (2000) *J. Neurosci.* **20,** RC96
7. Moita, M. A., Lamprecht, R., Nader, K., and LeDoux, J. E. (2002) *Nature Neurosci.* **5,** 837–838
8. Lamprecht, R., Farb, C. R., and LeDoux, J. E. (2002) *Neuron* **36,** 727–738
9. Matus, A. (2000) *Science* **290,** 754–758
10. Bonhoeffer, T., and Yuste, R. (2002) *Neuron* **35,** 1019–1027
11. Tamaskovic, R., Bichsel, S. J., and Hemmings, B. A. (2003) *FEBS Lett.* **546,** 73–80
12. Stegert, M. R., Tamaskovic, T., Bichsel, S. J., Hergovich, A., and Hemmings, B. A. (2004) *J. Biol. Chem.* **279,** 23806–23812
13. Devroe, E., Erdjument-Bromage, H., Tempst, P., and Silver, P. A. (2004) *J. Biol. Chem.* **279,** 24444–24451
14. Yoshikawa, T., Sanders, A. R., Esterling, L. E., Overhauser, J., Garnes, J. A., Lennon, G., Grewal, R., and Detera-Wadleigh, S. D. (1997) *Am. J. Med. Genet.* **74,** 140–149
15. Goslin, K., Asmussen, H., and Banker, G. (1998) in *Culturing Nerve Cells* (Banker, G., and Goslin, K., eds) pp 339–370, MIT Press, Cambridge, MA
16. Lamprecht, R., and LeDoux, J. E. (2003) *Nat. Rev. Neurosci.* **5,** 45–54
17. Geng, W., He, B., Wang, M., and Adler, P. N. (2000) *Genetics* **156,** 1817–1828
18. Zallen, J. A., Peckol, E. L., Tobin, D. M., and Bargmann, C. I. (2000) *Mol. Biol. Cell* **11,** 3177–3190
19. Altun-Gulteki, Z. F., Chandriani, S., Bougeret, C., Ishizaki, T., Narumiya, S., de Graaf, P., Van Bergen en Henegouwen, P., Hanafusa, H., Wagner, J. A., and Birge, R. B., (1998) *Mol. Cell. Biol.* **18,** 3044–3058
20. Pawlak, G., and Helfman, D. M. (2001) *Curr. Opin. Genet. Dev.* **11,** 41–47
21. Millward, T. A., Heizmann, C. W., Schäfer, B. W., and Hemmings, B. A. (1998) *EMBO J.* **17,** 5913–5922
22. Selinfreund, R. H., Barger, S. W., Welsh, M. J., and Van Eldik, L. J. (1990) *J. Cell Biol.* **111,** 2021–2028
23. Mikkelsen, S. E., Novitskaya, V., Kriajevska, M., Berezin, V., Bock, E., Norrild, B., and Lukanidin, E. (2001) *J. Neurochem.* **79,** 767–776
24. Huang, C. M., Tsay, K. E., and Kao, L. S. (1996) *J. Neurochem.* **67,** 530–539
25. Rusanescu, G., Qi, H., Thomas, S. M., Brugge, J. S., and Halegoua, S. (1995) *Neuron* **15,** 1415–1425
26. Ohta, Y., Akiyama, T., Nishida, E., and Sakai, H. (1987) *FEBS Lett.* **222,** 305–310
27. Prat, A. G., Bertorello, A. M., Ausiello, D. A., and Cantiello, H. F. (1993) *Am. J. Physiol.* **265,** 224–233
28. O'Malley, A., O'Connell, C., and Regan, C. M. (1998) *Neuroscience* **87,** 607–613
29. Geinisman, Z., Berry, R. W., Disterhoft, J. F., Power, J. M., and Van der Zee, E. A. (2001) *J. Neurosci.* **21,** 5568–5573

Available online at www.sciencedirect.com

SCIENCE DIRECT

Genomics 84 (2004) 1041–1050

GENOMICS

www.elsevier.com/locate/ygeno

Mitochondrial DNA 3644T→C mutation associated with bipolar disorder

Kae Munakata[a], Masashi Tanaka[b], Kanako Mori[a], Shinsuke Washizuka[a], Makoto Yoneda[c], Osamu Tajima[d], Tsuyoshi Akiyama[e], Shinichiro Nanko[f], Hiroshi Kunugi[g], Kazuyuki Tadokoro[g], Norio Ozaki[h], Toshiya Inada[h], Kaoru Sakamoto[i], Takako Fukunaga[i], Yoshimi Iijima[j], Nakao Iwata[k], Masahiko Tatsumi[l], Kazuo Yamada[m], Takeo Yoshikawa[m], Tadafumi Kato[a,*]

[a]*Laboratory for Molecular Dynamics of Mental Disorders, RIKEN Brain Science Institute, Hirosawa 2-1, Wako, Saitama 351-0198, Japan*
[b]*Department of Gene Therapy, Gifu International Institute of Biotechnology, Gifu, Japan*
[c]*Department of Internal Medicine, Fukui Medical University, Fukui, Japan*
[d]*Kyorin University School of Health Sciences, Kyorin, Japan*
[e]*Department of Neuropsychiatry, NTT East Kanto Medical Center, Kanto, Japan*
[f]*Department of Psychiatry, Teikyo University School of Medicine, Teikyo, Japan*
[g]*Department of Mental Disorder Research, National Institute of Neuroscience, Tokyo, Japan*
[h]*Department of Psychiatry, Faculty of Medicine, Nagoya University, Nagoya, Japan*
[i]*Department of Psychiatry, Tokyo Women's Medical College, Tokyo, Japan*
[j]*National Institute of Mental Health, National Center of Neurology and Psychiatry, Tokyo, Japan*
[k]*Department of Psychiatry, Faculty of Medicine, Fujita Health University, Fujita, Japan*
[l]*Department of Psychiatry, Faculty of Medicine, Showa University, Showa, Japan*
[m]*Laboratory for Molecular Psychiatry, RIKEN Brain Science Institute, Hirosawa 2-1, Wako, Saitama 351-0198, Japan*

Received 11 June 2004; accepted 18 August 2004
Available online 17 September 2004

Abstract

Mitochondrial dysfunction associated with mutant mitochondrial DNA (mtDNA) has been suggested in bipolar disorder, and comorbidity with neurodegenerative diseases was often noted. We examined the entire sequence of mtDNA in six subjects with bipolar disorder having comorbid somatic symptoms suggestive of mitochondrial disorders and found several uncharacterized homoplasmic nonsynonymous nucleotide substitutions of mtDNA. Of these, 3644C was found in 5 of 199 patients with bipolar disorder but in none of 258 controls ($p = 0.015$). The association was significant in the extended samples [bipolar disorder, 9/630 (1.43%); controls, 1/734 (0.14%); $p = 0.007$]. On the other hand, only 5 of 25 family members with this mutation developed bipolar disorder, of which 4 patients with 3644C had comorbid physical symptoms. The 3644T→C mutation converts amino acid 113, valine, to alanine in the NADH-ubiquinone dehydrogenase subunit I, a subunit of complex I, and 113 valine is well conserved from *Drosophila* to 61 mammalian species. Using transmitochondrial cybrids, 3644T→C was shown to decrease mitochondrial membrane potential and complex I activity compared with haplogroup-matched controls. According to human mitochondrial genome polymorphism databases, 3644C was not found in centenarians but was found in 3% of patients with Alzheimer disease and 2% with Parkinson disease. The result of modest functional impairment caused by 3644T→C suggests that this mutation could increase the risk for bipolar disorder.

Keywords: Bipolar disorder; MtDNA 3644T→C; Association study; Mitochondrial membrane potential; Complex I activity

Bipolar disorder is a major mental disorder characterized by recurrent manic and depressive episodes affecting about 1% of the population. The contribution of multiple genetic factors in the etiology of bipolar disorder is known from studies of twins, adoptions, and families. Although recent

* Corresponding author. Fax: +81 48 467 6947.
E-mail address: kato@brain.riken.go.jp (T. Kato).

0888-7543/$ - see front matter © 2004 Elsevier Inc. All rights reserved.
doi:10.1016/j.ygeno.2004.08.015

studies suggested several candidate polymorphisms, such as Val 311 of the brain-derived neurotrophic factor [1,2] and the −116G polymorphism of X-box binding protein 1 [3], the pathophysiological mechanisms of bipolar disorder have not yet been totally elucidated. Mitochondrial dysfunction in bipolar disorder was initially suggested by altered brain energy metabolism detected by ^{31}P magnetic resonance spectroscopy [4] and was recently supported by the altered gene expressions of mitochondria-related genes revealed by DNA microarray analysis in the postmortem brain [5]. The comorbidity of bipolar disorder or depression and a mitochondrial disorder, chronic-progressive external ophthalmoplegia (CPEO) [6–8], also suggests that mitochondrial dysfunction can cause bipolar disorder. It was pointed out that some families of bipolar disorder were seen in the maternal lineage [9], suggesting that mitochondrial DNA may have a pathophysiological role in bipolar disorder. The authors previously reported an association between bipolar disorder and two mitochondrial DNA (mtDNA) polymorphisms, 5178C and 10398A, in Japanese subjects [10]. A similar trend of association with 10398A was also reported in Caucasians [11]. These two polymorphisms convert amino acids in the subunits of complex I (NADH:ubiquinone oxidoreductase). NDUFV2, a nuclear-encoded complex I subunit gene, was also associated with bipolar disorder [12]. These results suggest that other genetic variations of complex I subunits in mtDNA are also risk factors for bipolar disorder.

Human mtDNA is inherited only maternally and encodes 13 protein subunits of the respiratory chain, including 7 complex I subunit genes, 22 tRNAs, and rRNAs [13]. It has been reported [14] that heteroplasmic tRNA mutations of mtDNA are related to neuromuscular diseases such as mitochondrial myopathy, encephalopathy, lactic acidosis and stroke-like episodes (MELAS), and myoclonus epilepsy with ragged-red fibers. Large-scale deletions are related to CPEO. On the other hand, there are missense mutations of mtDNA related to diseases, such as neurogenic muscle weakness, ataxia, and retinitis pigmentosa; Leigh encephalopathy; and Leber hereditary optic neuropathy (LHON). Most are heteroplasmic, a mixture of mutant and wild-type mtDNA, but sometimes these mutations can be homoplasmic in patients. The homoplasmic mutation of 1555A→G in the rRNA coding region related to inherited hearing loss caused by aminoglycoside toxicity is well described [15,16]. Alterations in mtDNA have also been studied in patients with Parkinson disease and Alzheimer disease [17,18]. The phenotypes of mitochondrial diseases are diverse and overlapping. The same mtDNA mutation can produce quite different phenotypes, while different mutations can produce similar phenotypes. The mutations or polymorphisms associated with bipolar disorder, if any, may also cause overlapping phenotypes and become a risk factor for other disorders.

In this study, we hypothesized that there are some homoplasmic mutations or polymorphisms increasing the risk for bipolar disorder and other signs and symptoms related to mitochondrial impairment. To identify such nucleotide substitutions of mtDNA, we sequenced the entire 16.6-kb mtDNA of patients with comorbidity of bipolar disorder and somatic symptoms frequently associated with mitochondrial disorders. Among newly identified nonsynonymous nucleotide substitutions in these patients, the 3644T→C at NADH-ubiquinone dehydrogenase subunit I (ND1), decreasing mitochondrial membrane potential and complex I activity, was associated with bipolar disorder. The comorbidity with bipolar disorder was present in most of these cases but their phenotypes were various. It was suggested that this mutation could increase risks for bipolar disorder with syndromic comorbidity.

Results and discussion

Unreported homoplasmic mtDNA base substitutions in patients

We examined the entire mtDNA sequence of six patients with bipolar disorder and somatic symptoms suggestive of mitochondrial disorders, such as ptosis, optic neuropathy, cardiomyopathy, and myoclonus (Table 1). None of them could be diagnosed as known mitochondrial diseases, such as MELAS, CPEO, and LHON, because of the reasons as described under Case reports. Five of them had a family history of mood disorder compatible with maternal inheritance. Every patient had several base substitutions compared with the revised Cambridge Reference Sequence [13,19]. The average number of base substitutions in each individual was 32.5 ± 6.9 (mean ± SD), and that of nonsynonymous base substitutions was 5.5 ± 2.1. We consulted the MITOMAP database (http://www.mitomap.org/) [20,21], and two mutations were provisionally reported in relation to mitochondrial diseases, 11084A→G (MELAS) and 12311T→C (CPEO). We also found four nonsynonymous nucleotide substitutions, 3644T→C, 4705T→C, 13651A→G, and 13928G→T, which were not registered in the MITOMAP, all of which were in the complex I subunits. We confirmed that these base substitutions were homoplasmic by the PCR restriction-length polymorphism method (PCR-RFLP).

To identify the mtDNA base substitutions having pathophysiological significance, we examined whether these base substitutions were found in 96 Japanese centenarians using the mtSNP database (Human Mitochondrial Genome Polymorphism Database in Japan, http://www.giib.or.jp/mtsnp/index_e.html) [22]. We regarded the base substitutions found in centenarians as having minimum pathophysiological significance. Base substitutions 4705T→C, 11084A→G, 12311T→C, and 13651A→G were found in centenarians, while two base substitutions, 3364T→C and 13928G→T, were not found in centenarians.

Table 1
Patients and unreported nucleotide substitutions of mitochondria DNA

Case	Diagnosis	Gender	Age at onset	Clinical manifestations		MtDNA substitutions	
				Physical symptoms	Family history	Unreported	Provisionally disease related
1	Bipolar I disorder	F	17	Optic neuritis	Mo, depression	13651A→G	
2	Bipolar I disorder	M	30	Cerebral infarction Dilated cardiomyopathy	Bro, bipolar disorder MoSib, psychotic NOS		
3	Bipolar I disorder	M	50	Ptosis Epilepsy Cardiac arrhythmia	MoSib, depression		12311T→C (CPEO)
4	Bipolar I disorder	F	24	Epileptic EEG	Bro, bipolar disorder Sis, NOS		11084A→G (MELAS)
5	Bipolar I disorder	M	57	Ptosis Muscle weakness NIDDM Multiple cerebral infarction	Sporadic	3644T→C	
6	Bipolar I disorder	M	35	Ptosis	Sib, depression	4705T→C 13928G→T	

Abbreviations: Mo, mother; Bro, brother; Sis, sister; Sib, sibling; MoSib, mother's sibling; psychotic NOS, psychotic disorder not otherwise specified.

Association study of mtDNA base substitutions

To know whether these two base substitutions, 3644T→C and 13928G→T, are associated with bipolar disorder, we used two sets of the study subjects. The initial association study consisted of 199 patients with bipolar disorder and 258 healthy volunteers. An additional independent sample set in COSMO (Collaborative Study of Mood Disorder) consisted of 431 patients with bipolar disorder and 476 healthy volunteers, was also used. To examine whether there is a hidden population structure, we performed stratification analysis on the initial samples using eight polymorphisms [3] using the method of Pritchard et al. [23], and no subpopulation was found for either patients or controls. We performed a similar stratification analysis using 20 SNPs in 169 Japanese samples, including COSMO samples, and found no subpopulation. We further analyzed the stratification in 169 Japanese samples using 374 microsatellite markers and found no hidden subpopulation (Yamada et al., manuscript in preparation). Thus, we concluded that there is no hidden subpopulation in our Japanese samples. Six patients examined for the entire mtDNA sequence were included in the first sample set, because they developed comorbid somatic symptoms after the diagnosis of bipolar disorder.

We genotyped at 3644 and 13928 by PCR-RFLP in the initial sample set (Table 2). Base 3644C was found in 5 of 199 Japanese patients with bipolar disorder in the first sample set, including the proband (case 5 in Table 1, II-1 of family A in Fig. 1), but in none of the controls ($p = 0.015$) (Table 2). Among other 4 patients, 1 had non-insulin-dependent diabetes mellitus (NIDDM), 1 had headache, and 1 had tremor suggestive of neurological impairment. In their family members, only 5 of 25 members in the same maternal lineages, who were assumed to have the same genotype, 3644C, developed

Table 2
Association study using independent sample sets and haplogroups

Base at 3644:	All samples					Haplogroup D (5178A/10398G)				
	T		C		p value	T		C		p value
Initial sample set										
Patients	97.5%	(194)	2.5%	(5)		94.4%	(68)	5.6%	(4)	
Controls	100.0%	(258)	0.0%	(0)	0.015*	100.0%	(97)	0.0%	(0)	0.003*
Independent sample set										
Patients	99.1%	(427)	0.9%	(4)		98.3%	(171)	1.7%	(3)	
Controls	99.8%	(475)	0.2%	(1)	0.197	100.0%	(192)	0.0%	(0)	0.106
Total sample set										
Patients	98.6%	(621)	1.4%	(9)		97.2%	(239)	2.8%	(7)	
Controls	99.9%	(733)	0.1%	(1)	0.007*	100.0%	(289)	0.0%	(0)	0.004*

Each number in parentheses shows the real number of subjects. The p value was given by Fisher's exact test.
* Statistically significant.

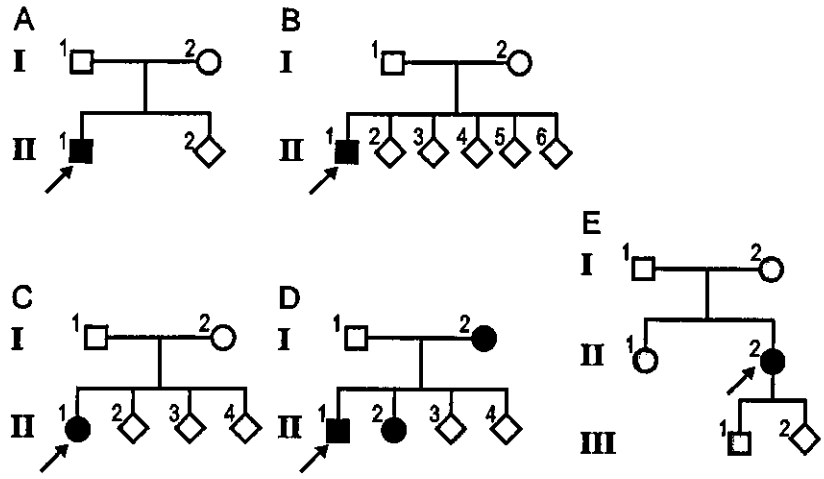

Fig. 1. Pedigrees of the probands with bipolar disorder and mitochondrial 3644C mutation. Arrows indicate the probands with bipolar disorder. Closed squares and circles indicate the patients with bipolar disorder or other mental disorders as follows: D, I-2 had a psychotic disorder not otherwise specified, II-2 had schizotypal personality disorder. Their comorbidities were as follows: A, II-1 had muscle weakness, ptosis, and NIDDM (case 5 in Table 1); C, II-1, had essential tremor; D, II-1, had NIDDM; E, I-2, II-1, II-2, and III-1 had headache. To maintain the anonymity of the pedigrees, the sexes of the unaffected siblings are not shown.

bipolar disorder, of which 4 patients with 3644C had comorbid physical symptoms and one had only bipolar disorder. Mutation 3644T→C converts amino acid 113 valine in the putative third transmembrane region of ND1, the protein subunit of complex I, to alanine. This 113 valine is well conserved from *Drosophila* to 61 mammalian species. There was no difference in the frequency of 13928G→T [13 of 199 patients with bipolar disorder (6.5%) and 19 of 258 controls (7.4%), $p = 0.804$ by Fisher's exact test]. Mutation 13928G→T changes the 531 serine into isoleucine in the ND5 subunit and it was not conserved even among mammalian species.

We further analyzed 3644T→C as a candidate risk factor for bipolar disorder using the independent sample set obtained from COSMO. While 4 additional individuals having 3644C were found among the patients, only 1 of the 476 controls had 3644C. Although this difference in frequency was not statistically significant ($p = 0.197$), this is likely due to the low statistical power to detect the difference (0.29). In the analysis of total samples having higher statistical power (0.79), 3644C was significantly more common in bipolar disorder than in the controls ($p = 0.007$) (Table 2).

Since mtDNA is highly polymorphic, other polymorphisms possibly confounded the association analysis. To minimize the effects of other polymorphisms, we categorized these samples into mitochondrial DNA haplogroups and the association analysis was repeated in each haplogroup. Seven patients with 3644C were assigned to the Asian haplogroup D characterized by 5178A/10398G [22], which we reported as an anti-risk haplotype for bipolar disorder [10]. The 3644C was significantly associated with bipolar disorder in haplogroup D (Table 2). On the other hand, only 1 control subject and 2 patients with 3644C were classified into haplogroup M characterized by 5178C/10398G, and no association was found in haplogroup M [2 of 187 patients (1.1%) and 1 of 233 controls (0.4%), $p = 0.588$].

We concluded that 3644C was associated with bipolar disorder for the following reasons: 3644T→C was associated with bipolar disorder in the initial case-control study; this substitution converts well-conserved amino acid 113 valine to alanine in ND1. A similar trend was observed in the independent samples, although there was no significant difference, possibly due to the small number of subjects replicating the association. In the analysis of the total sample set having enough statistical power to detect a difference, 3644C was significantly associated with bipolar disorder. The significant association between 3644C and bipolar disorder remained in haplogroup-matched case-control analysis.

We called 3644C a "mutation," because its frequency was very low (0.14% in 734 controls and 0.7% in 1364 total samples examined), it converted a well-conserved amino acid, and it appeared in at least two independent haplogroups. However, this mutation is not sufficient to cause bipolar disorder because 3644C was found in 1 healthy volunteer, and only 5 of 25 members in the same maternal lineages, all of whom were assumed to have 3644C, developed bipolar disorder. Among these patients, comorbidity in 4 patients with bipolar disorder was heterogeneous: 2 had NIDDM, 1 headache, and 1 tremor suggestive of neurological impairment. The other patient had only bipolar disorder. It means that 3644C cannot be a risk factor for comorbid symptoms seen in these patients but could be a risk factor for bipolar disorder, if not a causative mutation. Bipolar disorder is a multigenic disease and one type of mutation in mtDNA can cause various phenotypes. We

postulate that synergistic effects of other risk factors and 3644C could cause bipolar disorder.

Functional analyses in cybrids with 3644C

To evaluate the functional consequences of 3644T→C, we generated cell lines of the transmitochondrial hybrids, "cybrids," using the platelets derived from the subjects. Different from heteroplasmic mutations in the regions of tRNAs and protein subunits, functional impairment associated with homoplasmic mutation has not been well established. In the case of heteroplasmic mutation, two cybrid cell lines with different nucleotides at one particular position of mtDNA could be generated and analyzed. On the other hand, in the case of homoplasmic mutation, it was impossible to identify such a pair of cell lines. To minimize the effects of other polymorphisms, we compared cybrids with 3644C with haplogroup-matched controls for functional studies. A total of 24 cybrid cell lines were obtained from the initial sample set, and 9 cybrid cell lines belonged to haplogroup D, 5178A/10398G (Table 3). Among the 9 cell lines, only 2 were from patients with 3644C (II-1 in family D and II-2 in family E, in Fig. 1) and 7 were from subjects with 3644T (3 patients with bipolar disorder and 4 controls). We could not obtain other samples with 3644C because of ethical reasons.

Mitochondrial membrane potential (MMP) was measured using JC-1, a fluorescent cationic dye, which accumulates in mitochondria and changes its emission from wavelength 527 nm (monomer) to 590 nm (aggregates) depending on the mitochondrial membrane potential, and a fluorescence-activated cell sorter (FACS), and it distinguished well the difference between control cybrids and $\rho^0$206 cells lacking mtDNA: while 82.9 ± 9.9% (mean ± SD, N = 12) of the cybrids from control subjects were polarized, only 13.2 ± 7.7 (mean ± SE of three measurements) of the $\rho^0$206 cells were polarized (Fig. 2, left and right, respectively). This indicated that our measurement method is sensitive enough to detect the difference in MMP. The percentage of polarized cells was significantly decreased in cybrids with 3644C [51.7 ± 6.6 and 67.0 ± 4.3% (means ± SE), respectively] compared with haplogroup-matched cybrids (df = 8, p = 0.04 by Mann-Whitney U test) (Table 3). There was no significant difference between cybrids of bipolar disorder and controls nor between cybrids of other haplogroups.

Subsequently, the activities of complexes I (rotenone-insensitive), III, and IV in the electron-transport chain were measured using the citrate synthase activity as the reference (Table 4). The activity of $\rho^0$206 cells was measured to assess nonspecific activity. The 3644C group consisted of two cybrid cell lines. While there was no significant difference between complex III and complex IV activities ($p > 0.1$), complex I activity of the two cybrids with 3644C tended to be lower than four haplogroup-matched control cybrids (df = 5, p = 0.06 by Mann-Whitney U test). Decreased MMP could be explained by reduced complex I activity since MMP is maintained by the efflux of protons from the mitochondrial matrix, in which complex I plays an important role. MMP generated by the proton gradient is the driving force of not only ATP synthesis but also Ca^{2+} uptake across the mitochondrial inner membrane. We hypothesized that impaired mitochondrial Ca^{2+} uptake caused altered calcium signaling in bipolar disorder. Our result of decreased MMP in cybrids with 3644C supports our hypothesis.

Interestingly, the mtSNP database [22] showed that while 3644C was not found in 96 centenarians, it was found in 3.1% (3/96) of patients with Alzheimer disease and 2.0% (2/96) of patients with Parkinson disease. These findings suggested a possibility that 3644C is a risk factor common to bipolar disorder and neurodegenerative disorders, rather than a causative mutation only for bipolar disorder. If 3644C is also a risk factor for neurodegener-

Table 3
Mitochondrial membrane potential (MMP) of 24 cybrid cell lines

	N	Age	(C/B)	Gender	MMP
Diagnosis					
Control	12	48.0 ± 9.2		6/6	82.9 ± 9.9
Bipolar disorder	12	41.8 ±11.4		6/6	77.2 ±11.0
Bipolar disorder with 3644T	10	40.7 ±12.0		5/5	80.8 ± 7.0
Bipolar disorder with 3644C	2	42, 53		1/1	59.4 ±10.9*
Haplogroup					
10398A–5178C–3644T	7	43.6 ± 10.6	4/3	3/4	81.9 ± 8.6
10398G–5178C–3644T	8	41.6 ± 10.7	4/4	4/4	80.8 ± 9.5
10398G–5178A–3644T	7	48.9 ± 10.5	4/3	3/4	83.3 ± 8.5
10398G–5178A–3644C	2	42, 53	0/2	1/1	59.4 ±10.9**
ρ^0 cells	1				13.21

C/B, numbers of control/bipolar disorder; gender, number of men/women. The p value was given by the Mann–Whitney U test.
* p = 0.03 vs 3644T, 0.08 vs controls.
** p = 0.04 vs 3644T, 0.03 vs all other haplogroups.

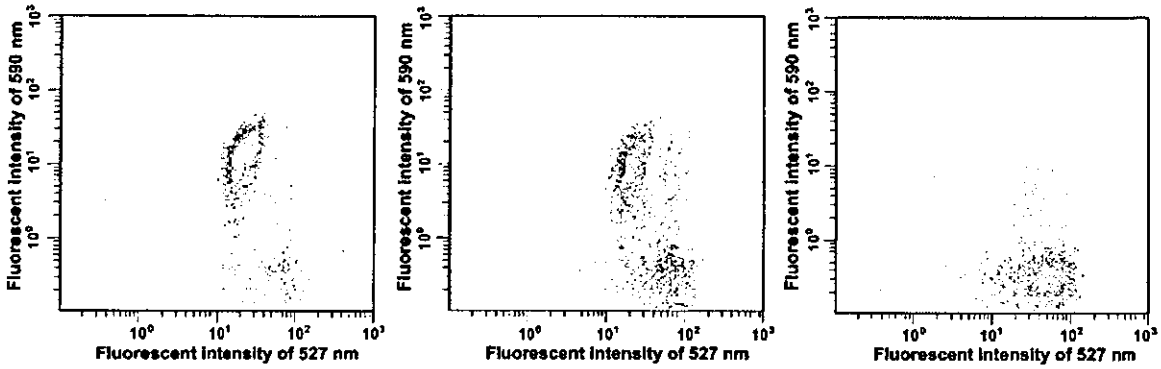

Fig. 2. Measurement of mitochondrial membrane potential using JC-1 and FACS. Vertical line, the fluorescence intensity of 590 nm, reflecting the aggregates and indicating high MMP. Horizontal line, the fluorescence intensity of 527 nm, reflecting the monomer and indicating low MMP. 10,000 cells were examined for one cell line. Representative results of one experiment each from three cell lines are shown. Left, control cybrids whose haplogroups were matched with the cybrids with 3644C; middle, cybrids with 3644C; right, $\rho^0$206 cells. While most control cybrids were polarized, having high 590/527 nm, most $\rho^0$206 cells were depolarized. The cybrids with 3644C were intermediate, having both polarized and depolarized cells.

ative disorders, the mechanism might be explained by a disruption of MMP that causes apoptosis. It is also compatible with the reduction of complex I activity in platelets or altered calcium signaling in cybrids derived from patients with Parkinson disease or Alzheimer disease [24–26]. Neuropathological studies of bipolar disorder also showed a decreased number of neurons in postmortem brains [27,28]. It was pointed out that having bipolar disorder increases the risk of Alzheimer disease [29,30] and Parkinson disease [31]. Two mood stabilizers, lithium and valproate, are known to have antiapoptotic effects by increasing Bcl-2 [32]. These findings are also compatible with the possibility that 3644C is a risk factor common to bipolar disorder and neurodegenerative disorders.

One might have a concern that 3644C is not a risk factor for bipolar disorder but associated with physical symptoms. Although the initial patient had several physical symptoms suggestive of mitochondrial disorder such as ptosis, muscle weakness, NIDDM, and cerebral infarction, other patients carrying 3644C had no or one nonspecific comorbid symptom. Thus, the apparent association between bipolar disorder and 3644C cannot be explained by the secondary phenomenon due to physical symptoms. However, it cannot be ruled out that these patients carrying 3644C have some subtle mitochondria-related symptoms that were not clinically apparent. In fact, there are reports of patients with pathogenic mtDNA mutations such as 3243A→G who showed psychotic symptoms at first and developed mitochondrial diseases later [33,34]. It might be possible that detailed physical examinations, for example, glucose tolerance test or close neurological examinations, would reveal subtle comorbid somatic symptoms. Needless to say, we need to address whether the 3664C substitution is associated with somatic symptoms alone. In the future, it is needed to look carefully at the phenotype and the clinical course of these subjects and investigate whether 3644C is associated with bipolar disorder or a bipolar disorder-somatic symptom subtype.

Functional impairment was reported also in the homoplasmic mutation, 1555A→G, in maternally inherited hearing loss [15,16]. The 11778A mutation of LHON, which is usually heteroplasmic but sometimes homoplasmic, was also shown to cause a modest reduction in complex I activity [35]. It was pointed out that the nuclear background potentially affects the expression of mtDNA polymorphisms [36]. Further study using cybrids with another nuclear background would be interesting. The mechanism of how the V113A amino acid substitution caused by 3644T→C in ND1 decreases complex I activity cannot be explained since the structure and function of each protein subunit are not yet well known. In particular, it remains unclear how complex I translocates protons across the mitochondrial inner membrane coupled to electron transfer. In summary, 3644T→C is a rare base substitution of mtDNA but induces modest impairment of complex I activity and becomes a risk factor for bipolar disorder.

Materials and methods

Subjects

Patients with bipolar disorder were diagnosed according to the DSM-III-R or DSM-IV criteria by at least two

Table 4
Enzyme activities of electron-transport chain of cybrids with 3644C and controls

	Control (mean ± SD), $N = 4$	3644C (mean ± SD), $N = 2$	ρ^0cells	p value*
Complex I/CS	14.47 ± 5.43	7.64 ± 0.08	4.82	0.06
Complex III/CS	32.15 ± 12.78	21.12 ± 2.72	7.36	0.36
Complex IV/CS	39.74 ± 11.24	29.21 ± 6.97	0.76	0.36

* The p value was calculated using the Mann–Whitney U test.

interview sessions by two senior psychiatrists and a consensus diagnosis was made. Their family history of mental disorder was assessed by interviewing the proband and available relatives. Control subjects were recruited from the staff or students of participating institutes and their friends, who reported themselves to be healthy. Written informed consent was obtained from all subjects. This study was approved by the ethics committees of RIKEN and all participating institutes.

The study subjects for the initial association study consisted of 199 patients with bipolar disorder (143 bipolar I and 56 bipolar II, 76 male and 123 female, 49.8 years of age on average) and 258 healthy volunteers (129 male and 129 female, 33.0 years of age on average). An additional independent sample set in COSMO consisted of 431 patients with bipolar disorder (214 male and 217 female, 49.5 years of age on average) and 476 healthy volunteers (226 male and 250 female, 50.4 years of age on average).

Six patients with bipolar disorder with somatic symptoms suggestive of mitochondrial disorders were chosen from the first sample set for examination of the entire mtDNA. They had been recruited in our bipolar disorder study based on our inclusion criteria, having DSM-IV bipolar disorder by consensus diagnoses after two nonstructured interview sessions with senior psychiatrists, and exclusion criteria, having no clinically remarkable neurological diseases, head trauma, or comorbid Axis II diagnoses. Characteristics of these six subjects are listed below and summarized in the Table 1.

The transmitochondrial cybrids for the following functional analyses were generated from 24 subjects in the initial samples, including two patients with 3644C.

Case reports

Case 1, 38-year-old female, is a patient with bipolar I disorder without psychotic features. She had the first episode of mania with psychomotor agitation and confusion at age 17. At age 27, she was admitted to a hospital due to bilateral optic neuritis. She had no other symptoms suggestive of multiple sclerosis. Her optic neuritis was improved by steroid therapy, and final diagnosis was idiopathic optic neuropathy. Because she had no relatives with optic neuropathy and her symptoms were reversible, Leber disease was not considered by the attendant ophthalmologist.

Case 2 is a 61-year-old male diagnosed as having bipolar I disorder. At age 30, he had the onset of mania with mood-incongruent psychotic features. At age 60, after being discharged from a psychiatric hospital, he was admitted to a hospital due to stroke. Brain imaging revealed infarctions in the cerebellum and the brain stem. During this hospitalization, chest X-ray showed enlarged heart and he was diagnosed as idiopathic dilated cardiomyopathy. He also had renal failure. His attendant physician did not suspect mitochondrial disease.

Case 3 is a 56-year-old male diagnosed with bipolar I disorder. At age 49, he had the onset of depression characterized by depressive mood, fatigability, retardation, insomnia, and suicidal thought. At age 52, he suddenly became manic. During this manic episode, he caused a motor vehicle accident. He was admitted to a psychiatric ward for the treatment of mania. After the first admission, he had generalized tonic clonic seizures. Although electroencephalography (EEG) recording showed no signs of epilepsy, he was clinically diagnosed as having epilepsy. At age 54, he complained of swollen eyelid, and medical examination did not show any signs of renal failure. He also complained of muscle weakness and had an episode of falling down due to muscle weakness. A neurologist saw this patient and assessed that ptosis may be present but fluctuating and was not pathological. He also showed some tendency of disturbed movement of the eyes, but it was also fluctuating and he did not have diplopia. Muscle weakness was not objectively present. Based on these clinical examinations, the neurologist ruled out mitochondrial disease from differential diagnosis and judged that further investigation was not necessary. Electrocardiogram indicated supraventricular extrasystole, but it was not clinically remarkable.

Case 4 is a 46-year-old female diagnosed with bipolar I disorder. At age 24, she had the onset of mania. At age 40, she began rapid cycling. During her psychiatric hospitalization, EEG recording showed epileptic abnormality. However, she did not have any signs or symptoms of epilepsy and was not diagnosed as epileptic.

Case 5 is 57-year-old male diagnosed as having bipolar I disorder. He had the onset of a manic episode at age 50. Since his clinical representation resembled confusion caused by organic mental disorder, he received lumbar puncture by a neurologist during psychiatric hospitalization, which showed elevated cerebrospinal fluid protein levels. The neurologist also noted muscle weakness and slight ptosis on the left eyelid. However, these symptoms were improved without any treatment and his subsequent manic episodes were typical manic syndrome without any additional neurological features or psychotic features. He was finally diagnosed as having bipolar I disorder. After the onset of bipolar disorder, he was diagnosed as having non-insulin-dependent diabetes mellitus. His cranial magnetic resonance image showed multiple subcortical silent infarction.

Case 6 is a 38-year-old male having bipolar I disorder. His clinical record was published elsewhere [37]. He complained of ptosis during antipsychotic treatment. Both a neurologist and an ophthalmologist examined and diagnosed him as not having any mitochondrial disease, since his sign was transient and not clinically remarkable.

MtDNA sequencing

Total DNA was extracted from peripheral blood leukocytes by standard protocols. Entire mtDNA sequenc-

ing was performed as previously described [38] with some modifications. In short, each DNA sample was diluted to 10 μg/ml, and nested PCR was performed. PCR was initially performed to obtain two long PCR products, 6 and 11 kb of mtDNA; the second PCR was designed as a set of three overlapping fragments from the first 6-kb PCR product and six fragments from the first 11-kb PCR product. After the second PCR, the products were treated with a SeqDirect PCR Cleaning kit (Qbiogene, Carlsbad, CA, USA) according to the manufacturer's protocol. Both strands of these fragments were then sequenced with the BigDye Terminator Cycle Sequencing kit (Applied Biosystems, Foster City, CA, USA) and ABI Prism 3700 DNA sequencer (Applied Biosystems). Each mtDNA site was read at least three times, including at least once for each strand.

Genotyping

The two base substitutions of mtDNA, 3644T→C and 13928G→T, were genotyped using the PCR-RFLP method and sequencing. The enzymes and experimental conditions for the PCR-RFLP were as follows: 3644 was genotyped by primers 5′-GTAGAATGATGGCTAGGGTGACT-3′ and 5′-TCTAGCCACCTCTAGCCTAGACG-3′ and the restriction enzyme *Tai*I (Fermentas), 13928 by 5′-CATACTCGGATTC-TACGCTA-3′, 5′-TTTAGGTAATAGCTTTTCTA-3′, and *Nhe*I (Takara Bio, Inc., Shiga, Japan). MtDNAs 5178C→A and 10398A→G were genotyped to determine the haplogroups. Genotypes of 5178C→A and 10398A→G were examined as previously described [10].

Generation of cybrids

The 143B.TK$^-$ $\rho^0$206 cell line, lacking mtDNA and established by King and Attardi [39], was used for generating cybrids. Platelets of patients and controls were separated from peripheral blood and fused with $\rho^0$206 cells using 40% polyethylene glycol 1500 (Sigma), as previously described [40]. We used DMEM (Gibco BRL) containing 10% FBS (fetal bovine serum; Gibco BRL), penicillin/streptomycin, pyruvate (Gibco BRL), and uridine (Sigma) as the growth medium for ρ^0 cells. For the selection of transmitochondrial cybrid cell lines, we used DMEM containing 10% dialyzed FBS, penicillin/streptomycin, and pyruvate. After the harvest of individual cybrid cell lines, the integration of mtDNA was confirmed by Southern blot analysis using 18S ribosomal RNA repeating units as a reference [41]. The identity of the mtDNA of the cybrids with that of the donor was verified by sequencing the D loop and genotyping several polymorphisms. For Southern blot analysis, we used the ECL Labeling and Detection System according to the manufacturer's protocol (Amersham Biosciences Corp., NJ, USA). Cybrids were stored in liquid nitrogen for further experiments.

Measurement of MMP using JC-1

MMP was estimated using JC-1 (Molecular Probes, Eugene, OR) and flow cytometry. Cybrids stored in liquid nitrogen were thawed and incubated in an atmosphere of 5% CO_2 at 37°C in DMEM containing 10% FBS, penicillin/streptomycin, and pyruvate. Cells (1×10^6) were trypsinized and harvested in 10 ml of DMEM containing 10% FBS, washed with PBS (phosphate-buffered saline) once, and stained with DMEM containing 5 μg/ml JC-1 for 15 min at 37°C. Cells were then washed with PBS and subjected to analysis using a FACS (Epics Elite cell sorter; Beckman Coulter, Fullerton, CA, USA) as previously described [42]. The excitation wavelength was 488 nm by argon ion laser. Emissions at 590 and 527 nm were isolated by each photomultiplier detector and 10,000 cells were measured for each experiment. The experiment was performed in triplicate for each cell line. The cells with polarized mitochondria were defined by an intensity ratio of 590 nm/527 nm above 0.2.

Activities of enzymes in the electron-transport chain

For the sample preparation of the mitochondrial fraction, each line of cybrids was amplified until the cell count was 5×10^7. Cybrids were trypsinized and harvested in DMEM. After being washed once with PBS and once with isolation buffer [210 mM D-mannitol, 71 mM sucrose, 1 mM EGTA, 0.5% bovine serum albumin (fatty acid free), 5 mM Hepes, pH 7.2], the cells were suspended in 5 ml of isolation buffer. Using a chilled Dounce glass homogenizer with a loose fitting pestle, 20 passes were applied to the cell suspension on ice, which was centrifuged at 700*g* for 7 min at 4°C. The supernatant was centrifuged at 10,000*g* for 7 min at 4°C, and the mitochondrial pellet was obtained. The pellet was suspended in 250 mM sucrose, divided into aliquots, and kept at −80°C until use. Activities of complexes I, III, and IV were measured as previously described [43]. Rotenone-sensitive complex I activity was measured by the change in absorption of decylubiquinone. All samples were measured within 1 month from preparation. The activity of each complex was corrected by citrate synthase activity. All the chemical products for these assays were obtained from Sigma. We used a UVmini1240 spectrophotometer (Shimadzu, Kyoto, Japan) for this experiment.

Acknowledgments

We thank all the volunteers who participated in this study. We express our thanks to the members of the Research Resource Center at the RIKEN Brain Science Institute, especially to Mr. Miyazaki for the sequence procedure and to Mr. Ohtawa for the analysis of mitochondrial membrane potential. The 143B.TK$^-$ $\rho^0$206 cell line was a gift from Dr. Giuseppe Attardi to Dr. Makoto Yoneda.

References

[1] P. Sklar, S.B. Gabriel, M.G. McInnis, P. Bennett, Y.M. Lim, G. Tsan, S. Schaffner, G. Kirov, I. Jones, M. Owen, et al., Family-based association study of 76 candidate genes in bipolar disorder: BDNF is a potential risk locus. Brain-derived neurotrophic factor, Mol. Psychiatry 7 (2002) 579–593.

[2] M. Neves-Pereira, E. Mundo, P. Muglia, N. King, F. Macciardi, J.L. Kennedy, The brain-derived neurotrophic factor gene confers susceptibility to bipolar disorder: evidence from a family-based association study, Am. J. Hum. Genet. 71 (2002) 651–655.

[3] C. Kakiuchi, K. Iwamoto, M. Ishiwata, M. Bundo, T. Kasahara, I. Kusumi, T. Tsujita, Y. Okazaki, S. Nanko, H. Kunugi, et al., Impaired feedback regulation of XBP1 as a genetic risk factor for bipolar disorder, Nat. Genet. 35 (2003) 171–175.

[4] T. Kato, S. Takahashi, T. Shioiri, T. Inubushi, Alterations in brain phosphorous metabolism in bipolar disorder detected by in vivo ^{31}P and ^{7}Li magnetic resonance spectroscopy, J. Affect. Disord. 27 (1993) 53–59.

[5] C. Konradi, M. Eaton, M.L. MacDonald, J. Walsh, F.M. Benes, S. Heckers, Molecular evidence for mitochondrial dysfunction in bipolar disorder, Arch. Gen. Psychiatry 61 (2004) 300–308.

[6] G. Siciliano, A. Tessa, S. Petrini, M. Mancuso, C. Bruno, G.S. Grieco, A. Malandrini, L. DeFlorio, B. Martini, A. Federico, et al., Autosomal dominant external ophthalmoplegia and bipolar affective disorder associated with a mutation in the ANT1 gene, Neuromuscul. Disord. 13 (2003) 162–165.

[7] J.N. Spelbrink, F.Y. Li, V. Tiranti, K. Nikali, Q.P. Yuan, M. Tariq, S. Wanrooij, N. Garrido, G. Comi, L. Morandi, et al., Human mitochondrial DNA deletions associated with mutations in the gene encoding Twinkle, a phage T7 gene 4-like protein localized in mitochondria, Nat. Genet. 28 (2001) 223–231.

[8] G. Van Goethem, B. Dermaut, A. Lofgren, J.J. Martin, C. Van Broeckhoven, Mutation of POLG is associated with progressive external ophthalmoplegia characterized by mtDNA deletions, Nat. Genet. 28 (2001) 211–212.

[9] F.J. McMahon, O.C. Stine, D.A. Meyers, S.G. Simpson, J.R. DePaulo, Patterns of maternal transmission in bipolar affective disorder, Am. J. Hum. Genet. 56 (1995) 1277–1286.

[10] T. Kato, H. Kunugi, S. Nanko, N. Kato, Mitochondrial DNA polymorphisms in bipolar disorder, J. Affect. Disord. 62 (2001) 151–164.

[11] F.J. McMahon, Y.S. Chen, S. Patel, J. Kokoszka, M.D. Brown, A. Torroni, J.R. DePaulo, D.C. Wallace, Mitochondrial DNA sequence diversity in bipolar affective disorder, Am. J. Psychiatry 157 (2000) 1058–1064.

[12] S. Washizuka, C. Kakiuchi, K. Mori, H. Kunugi, O. Tajima, T. Akiyama, S. Nanko, T. Kato, Association of mitochondrial complex I subunit gene NDUFV2 at 18p11 with bipolar disorder, Am. J. Med. Genet. 120B (2003) 72–78.

[13] S. Anderson, A.T. Bankier, B.G. Barrell, M.H. de Bruijn, A.R. Coulson, J. Drouin, I.C. Eperon, D.P. Nierlich, B.A. Roe, F. Sanger, et al., Sequence and organization of the human mitochondrial genome, Nature 290 (1981) 457–465.

[14] D.C. Wallace, Mitochondrial diseases in man and mouse, Science 283 (1999) 1482–1488.

[15] T.R. Prezant, J.V. Agapian, M.C. Bohlman, X. Bu, S. Oztas, W.Q. Qiu, K.S. Arnos, G.A. Cortopassi, L. Jaber, J.I. Rotter, et al., Mitochondrial ribosomal RNA mutation associated with both antibiotic-induced and non-syndromic deafness, Nat. Genet. 4 (1993) 289–294.

[16] M.X. Guan, N. Fischel-Ghodsian, G. Attardi, Biochemical evidence for nuclear gene involvement in phenotype of non-syndromic deafness associated with mitochondrial 12S rRNA mutation, Hum. Mol. Genet. 5 (1996) 963–971.

[17] S.W. Chang, D. Zhang, H.D. Chung, H.P. Zassenhaus, The frequency of point mutations in mitochondrial DNA is elevated in the Alzheimer's brain, Biochem. Biophys. Res. Commun. 273 (2000) 203–208.

[18] J.M. van der Walt, K.K. Nicodemus, E.R. Martin, W.K. Scott, M.A. Nance, R.L. Watts, J.P. Hubble, J.L. Haines, W.C. Koller, K. Lyons, et al., Mitochondrial polymorphisms significantly reduce the risk of Parkinson disease, Am. J. Hum. Genet. 72 (2003) 804–811.

[19] R.M. Andrews, I. Kubacka, P.F. Chinnery, R.N. Lightowlers, D.M. Turnbull, N. Howell, Reanalysis and revision of the Cambridge reference sequence for human mitochondrial DNA, Nat. Genet. 23 (1999) 147.

[20] A.M. Kogelnik, M.T. Lott, M.D. Brown, S.B. Navathe, D.C. Wallace, MITOMAP: a human mitochondrial genome database, Nucleic Acids Res. 24 (1996) 177–179.

[21] A.M. Kogelnik, M.T. Lott, M.D. Brown, S.B. Navathe, D.C. Wallace, MITOMAP: a human mitochondrial genome database—1998 update, Nucleic Acids Res. 26 (1998) 112–115.

[22] M. Tanaka, T. Takeyasu, N. Fuku, G. Li-Jun, M. Kurata, Mitochondrial genome single nucleotide polymorphisms and their phenotypes in the Japanese, Ann. N. Y. Acad. Sci. 1011 (2004) 1–20.

[23] J.K. Pritchard, M. Stephens, P. Donnelly, Inference of population structure using multilocus genotype data, Genetics 155 (2000) 945–959.

[24] Y. Aomi, C.S. Chen, K. Nakada, S. Ito, K. Isobe, H. Murakami, S.Y. Kuno, M. Tawata, R. Matsuoka, H. Mizusawa, J.-I. Hayashi, Cytoplasmic transfer of platelet mtDNA from elderly patients with Parkinson's disease to mtDNA-less HeLa cells restores complete mitochondrial respiratory function, Biochem. Biophys. Res. Commun. 280 (2001) 265–273.

[25] R.H. Swerdlow, J.K. Parks, J.N. Davis II, D.S. Cassarino, P.A. Trimmer, L.J. Currie, J. Dougherty, W.S. Bridges, J.P. Bennett Jr., G.F. Wooten, W.D. Parker, Matrilineal inheritance of complex I dysfunction in a multigenerational Parkinson's disease family, Ann. Neurol. 44 (1998) 873–881.

[26] J.P. Sheehan, R.H. Swerdlow, S.W. Miller, R.E. Davis, J.K. Parks, W.D. Parker, J.B. Tuttle, Calcium homeostasis and reactive oxygen species production in cells transformed by mitochondria from individuals with sporadic Alzheimer's disease, J. Neurosci. 17 (1997) 4612–4622.

[27] M.P. Vawter, W.J. Freed, J.E. Kleinman, Neuropathology of bipolar disorder, Biol. Psychiatry 48 (2000) 486–504.

[28] G. Rajkowska, Cell pathology in bipolar disorder, Bipolar Disord. 4 (2002) 105–116.

[29] L.V. Kessing, E.W. Olsen, P.B. Mortensen, P.K. Andersen, Dementia in affective disorder: a case-register study, Acta Psychiatr. Scand. 100 (1999) 176–185.

[30] R.C. Green, L.A. Cupples, A. Kurz, S. Auerbach, R. Go, D. Sadovnick, R. Duara, W.A. Kukull, H. Chui, T. Edeki, et al., Depression as a risk factor for Alzheimer disease: the MIRAGE Study, Arch. Neurol. 60 (2003) 753–759.

[31] F.M. Nilsson, L.V. Kessing, T.G. Bolwig, Increased risk of developing Parkinson's disease for patients with major affective disorder: a register study, Acta Psychiatr. Scand. 104 (2001) 380–386.

[32] G. Chen, W.Z. Zeng, P.X. Yuan, L.D. Huang, Y.M. Jiang, Z.H. Zhao, H.K. Manji, The mood-stabilizing agents lithium and valproate robustly increase the levels of the neuroprotective protein bcl-2 in the CNS, J. Neurochem. 72 (1999) 879–882.

[33] E.C. Thomeer, W.M. Verhoeven, C.J. van de Vlasakker, J.L. Klompenhouwer, Psychiatric symptoms in MELAS: a case report, J. Neurol. Neurosurg. Psychiatry 64 (1998) 692–693.

[34] M. Yamazaki, H. Igarashi, M. Hamamoto, T. Miyazaki, I. Nonaka, A case of mitochondrial encephalomyopathy with schizophrenic psychosis, dementia and neuroleptic malignant syndrome, Rinsho Shinkeigaku 31 (1991) 1219–1223.

[35] M.D. Brown, I.A. Trounce, A.S. Jun, J.C. Allen, D.C. Wallace, Functional analysis of lymphoblast and cybrid mitochondria containing the 3460, 11778, or 14484 Leber's hereditary optic neuropathy mitochondrial DNA mutation, J. Biol. Chem. 275 (2000) 39831–39836.

[36] P.L. Roubertoux, F. Sluyter, M. Carlier, B. Marcet, F. Maarouf-Veray, C. Cherif, C. Marican, P. Arrechi, F. Godin, M. Jamon, et al., Mitochondrial DNA modifies cognition in interaction with the nuclear genome and age in mice, Nat. Genet. 35 (2003) 65–69.

[37] T. Kato, Y. Takahashi, Deletion of leukocyte mitochondrial DNA in bipolar disorder, J. Affect. Disord. 37 (1996) 67–73.

[38] J. Akanuma, K. Muraki, H. Komaki, I. Nonaka, Y. Goto, Two pathogenic point mutations exist in the authentic mitochondrial genome, not in the nuclear pseudogene, J. Hum. Genet. 45 (2000) 337–341.

[39] M.P. King, G. Attardi, Human cells lacking mtDNA: repopulation with exogenous mitochondria by complementation, Science 246 (1989) 500–503.

[40] A. Chomyn, S.T. Lai, R. Shakeley, N. Bresolin, G. Scarlato, G. Attardi, Platelet-mediated transformation of mtDNA-less human cells: analysis of phenotypic variability among clones from normal individuals—and complementation behavior of the tRNALys mutation causing myoclonic epilepsy and ragged red fibers, Am. J. Hum. Genet. 54 (1994) 966–974.

[41] I. Nishino, O. Kobayashi, Y. Goto, M. Kurihara, K. Kumagai, T. Fujita, K. Hashimoto, S. Horai, I. Nonaka, A new congenital muscular dystrophy with mitochondrial structural abnormalities, Muscle Nerve 21 (1998) 40–47.

[42] A. Sawa, G.W. Wiegand, J. Cooper, R.L. Margolis, A.H. Sharp, J.F. Lawler Jr., J.T. Greenamyre, S.H. Snyder, C.A. Ross, Increased apoptosis of Huntington disease lymphoblasts associated with repeat length-dependent mitochondrial depolarization, Nat. Med. 5 (1999) 1194–1198.

[43] I.A. Trounce, Y.L. Kim, A.S. Jun, D.C. Wallace, Assessment of mitochondrial oxidative phosphorylation in patient muscle biopsies, lymphoblasts, and transmitochondrial cell lines, Methods Enzymol. 264 (1996) 484–509.